

Discovery of small-molecule inhibitors of Rad6 function and the Rad6-Rad18 interaction

Ph.D. Dissertation

Gaurav Sharma

Supervisor: Lajos Haracska, Ph.D., D.Sc.



Doctoral School of Biology

University of Szeged

Institute of Genetics,
Biological Research Centre, Szeged
Szeged, 2023

Table of Contents

Table of Contents

List of Abbreviations	4
1. Introduction	6
1.1. DNA damage tolerance/bypass	9
1.2. PCNA	14
1.3. The role of Rad6	16
2. Goals and Objectives	19
3. Materials and Methods	20
3.1. FLAG-PCNA	20
3.2. GST-Flag-Uba1	20
3.3. FLAG-Ubr1	20
3.4. FLAG- Rad6, FLAG-Rad18, FLAG-UBC13 and FLAG-MMS2	21
3.5. GFP-Rad6 and GFP-Rad18	21
3.6. Rad6-Rad18 dimer	21
3.7. GST-Ubiquitin	22
3.8. His-Uba1	22
3.9. RFC complex	23
3.10. Plasmids, antibodies, and other reagents	24
3.11. Alpha assays	24
3.12. PCNA ubiquitination	25
3.13. Uba1~ubiquitin thioester formation	26
3.14. Rad6~ubiquitin thioester formation	26
3.15. Rad18 autoubiquitination	26
3.16. Rad6–Rad18 interaction	27
3.17. Mms2–Ubc13~ubiquitin thioester formation	27
3.18. Microscale thermophoresis	27
3.19. Rad6–Ubr1 pull-down	28
3.20. Rad6–Ubr1 interaction alpha assay	28
3.21. Cell culture	28
3.22. Cell survival	28
3.23. Computational docking of compounds to Rad6	29
3.24. QUANTIFICATION AND STATISTICAL ANALYSIS	30

4. Results and conclusion	31
4.1. Development and optimisation of ALPHA-based PCNA ubiquitination assay for high-throughput screening.	31
4.2. Development and optimisation of Rad6–Rad18 interaction assay	33
4.3. Screening for inhibitors of PCNA ubiquitination	33
4.4. Certain xanthenes and a related acridine derivative inhibit PCNA ubiquitination	35
4.5. Dose-response analysis for different compounds in PCNA ubiquitination	36
4.6. Dose-response analysis for Rad6~ubiquitin thioester formation	39
4.7. Dose–response for the Rad6–Rad18 interaction in the presence of compounds.	42
4.8. Confirming target-protein binding using microscale thermophoresis (MST)	45
4.9. Dose-response analysis of cell survival	47
4.10. Identification of possible compound-binding sites	48
5. Discussion	51
6. Summary	57
7. Összefoglaló	59
8. Acknowledgment	62
9. References	64
10. List of Publications	75
11. Declaration	76
12. Co-authors Declaration	77
13. Appendix	78

List of Abbreviations

ATP: Adenosine triphosphate

ALPHA: Amplified luminescent proximity homogeneous

BER: Base excision repair

Bio-Ub: Biotin-ubiquitin

CI: Confidence interval

DMSO: Dimethyl sulfoxide

DNA: Deoxyribonucleic acid

DSB: Double-strand break

DTT: Dithiothreitol

EDTA: Ethylenediaminetetraacetic acid

ELISA: Enzyme-linked immune sorbent assay

FBS: Fetal bovine serum

FRET: Fluorescence resonance energy transfer

GST: Glutathione S-transferase

GFP: Green fluorescent protein

HLTF: Helicase-like transcription factor

HRP: Horseradish peroxidase

HR: Homologous recombination

HTS: High throughput screening

IC50: Half maximal inhibitory concentration

IDCL: Interdomain-connecting loop

IPTG: Isopropyl- β -D-thiogalactoside

K164: Lysine 164 residue of PCNA

Kd: Dissociation constant

MMR: Mismatch repair

N/A: Not applicable

NSC 9037: C₁₉H₁₂O₆

NSC 80693: C₂₁H₁₇NO₅

NSC 119891: C₂₀H₁₂O₅

NSC 119888: $C_{20}H_{12}O_5$

NSC 157411: $C_{20}H_{16}O_5$

NSC 348718: $C_{22}H_{20}O_6$

NSC 71947: $C_{21}H_{19}N_3$

NHEJ: Non-homologous end joining

NMR: Nuclear magnetic resonance

PCNA: Proliferative cell nuclear antigen

RFC: Replication factor C

RING: Really Interesting New Gene

RNA: Ribonucleic acid

S phase: Synthesis phase

S/B: Signal-to-background ratio

SD: Standard deviation

S/N: Signal-to-noise ratio

SAR: Structure-activity relationship

SE: Standard error

SHPRH: Smf2 histone linker PHD ring helicase

SSMD: strictly standardized mean difference

STD: Saturation transfer difference

SUMO: Small ubiquitin-like modifier

TLS: Translesion synthesis

Uba1: Ubiquitin-activating enzyme 1

UBL: Ubiquitin like proteins

1. Introduction

Preserving genetic information during DNA replication is the most important task for dividing cells. However, cells constantly undergo multiple genotoxic alterations, which can result in genetic mutations that could cause cancer. Upon DNA damage, lesions can be left unrepaired from classical DNA repair mechanisms and these damages can stall the replication fork during the S-phase of the cell cycle. Cancer remains a precarious health issue even after decades of research to find its treatment. Traditional approaches to treat cancer constitute chemotherapy, radiotherapy, and surgical removal of the solid tumor, but chemotherapy's inability to distinguish between cancerous and normal cells results in significant toxicity and side effects, representing major drawbacks. Drugs based on small molecules are generally chemical compounds with a molecular weight < 900 Da, and – due to their small size – they tend to easily translocate through the plasma membrane and interact with the cytoplasmic domain of cell surface receptors and intracellular signaling molecules. Here, we focused on small molecules specifically targeting the post-translational modification of proliferating cell nuclear antigen (PCNA) by ubiquitin.

Certain proteins undergo a post-translational modification called ubiquitination, which involves attaching ubiquitin (a small protein) or a ubiquitin-like (UBL) protein to a target protein. This modification not only regulates the degradation of proteins by the proteasome (a cellular structure that breaks down proteins) but also plays a role in numerous other cellular processes. The attachment of ubiquitin or a UBL protein to a target protein acts as a tag or docking site for interactions with other proteins and the formation of large protein complexes, which are involved in signalling physiological events.

One protein known to interact with ubiquitin is proliferating cell nuclear antigen (PCNA), and ubiquitination can control many of these post-translational modifications (Yang et al., 2013). PCNA forms complexes that are involved in normal DNA replication (the “replisome”) or in a process called translesion synthesis (TLS), which can result in mutagenesis (the “mutasome”). A mutasome is a complex of proteins involved in the process of DNA damage repair. It is formed in response to DNA damage, particularly DNA double-strand breaks. The mutasome is responsible for recruiting and coordinating the activity of other repair factors, including endonucleases, helicases, and polymerases, to process and repair the damaged DNA. However, there are many different types of PCNA-based complexes with specialised functions. Compounds with selective bioactivity targeting the post-translational modification cascades involved in specific stages of a reaction series would serve as a valuable resource for studying the formation of these various complexes, as well as having considerable therapeutic applications. Ubiquitination of PCNA at lysine residue K164 acts as a trigger for DNA damage tolerance pathways. DNA damage tolerance pathways are cellular mechanisms that allow cells to temporarily tolerate or bypass DNA damage, allowing them to continue replicating their DNA in the presence of damage. This can be accomplished through several processes, including translesion synthesis (TLS) and template switching. PCNA binds to and coordinates the activities of various proteins, including DNA polymerases and other factors involved in DNA replication, repair, and regulation. After binding to DNA through ATP-dependent replication factor C (RFC), PCNA can be monoubiquitinated by the ubiquitin-conjugating enzyme E2 Rad6 in the ubiquitin ligase complex E3 Rad18. E2 Rad6 catalyses the reaction, while Rad18 serves as the adapter for specific substrate recognition in the reaction. The ubiquitination reaction cascade begins with

the ATP-dependent activation of the carboxyl terminus of ubiquitin, which is catalysed by the ubiquitin-activating enzyme E1 Uba1. This creates an adenylated ubiquitin intermediate that reacts with a specific cysteine residue in Uba1 to produce a high-energy Uba1-ubiquitin conjugate with a thioester bond. The ubiquitin moiety is then transferred to Rad6 to form a Rad6-ubiquitin thioester conjugate, which is present in a complex with Rad18. This complex then reacts with the side chain amine K164 on PCNA to form a more stable PCNA-ubiquitin bond. The activity of the Rad6–Rad18 complex is regulated by several other factors reviewed (Hedglin and Benkovic, 2015). Ubiquitination events have functions beyond targeting proteins for degradation by the proteasome, such as providing binding sites for protein-protein interactions. Rad18, a protein involved in DNA damage repair, can undergo autoubiquitination on multiple lysine residues, which may affect its function, subcellular localization, and stability against proteasomal degradation. (Miyase et al., 2005; Zeman et al., 2014).

The interaction between Rad6 and Rad18 involves the RING domain of Rad18, located near its N-terminus (Huang et al., 2011; Masuda et al., 2012; Notenboom et al., 2007), and the Rad6-binding domain (Rad6BD) on Rad18, near its C-terminus (Bailly et al., 1997; Huang et al., 2011; Notenboom et al., 2007). Rad6BD binds a region overlapping with the noncovalent ubiquitin-binding site of Rad6 (Huang et al., 2011).

In a recent study (Fenteany et al., 2020), we developed and optimised high-throughput assays to identify chemical modulators of the PCNA ubiquitination cascade. We identified a series of xanthenes as first-in-class probes of the Rad6 function and the association of Rad6 and Rad18. This is a significant discovery, as it reveals a new inhibitory activity for a small molecule in the PCNA ubiquitination cascade. These xanthenes have the potential as therapeutic agents for cancer treatment. Xanthenes

are organic molecules with a distinctive chemical structure. They consist of a benzene ring, a six-carbon ring with alternating double bonds, and a carbonyl group, a carbon atom covalently bound to an oxygen atom. Additionally, xanthenes have a side chain composed of two carbon atoms. They can be used as pigments, fluorescent markers, and dyes, for example. Xanthenes are also utilized in biology, material science, and electronics due to their unique characteristics, such as fluorescence, high reactivity, and the ability to form stable complexes with metal ions.

1.1. DNA damage tolerance/bypass

Deoxyribonucleic acid (DNA) is the biomolecule that acts as the genetic blueprint for all cellular life. It encodes the information required for an organism's development, growth, and physiological processes. DNA can be damaged by a number of factors, such as ionising radiation, ultraviolet light, and chemicals. Damage in DNA can lead to mutations and chromosomal rearrangements, which can cause genome instability and various diseases, including cancer. There exists a multitude of forms in which DNA lesions can occur, which includes apurinic/apyrimidinic (AP) sites commonly referred to as abasic sites, adducts, single-strand breaks (SSBs), double-strand breaks (DSBs), DNA-protein cross-links, as well as insertion/deletion mismatches (Rao et al., 1993). The cellular metabolic processes, along with temperature variations, errors in DNA replication and repair, and methylation, are responsible for the generation of endogenous agents such as reactive oxygen species (ROS) and reactive nitrogen species (RNS) (Figure 1) (Lindahl et al., 1993).

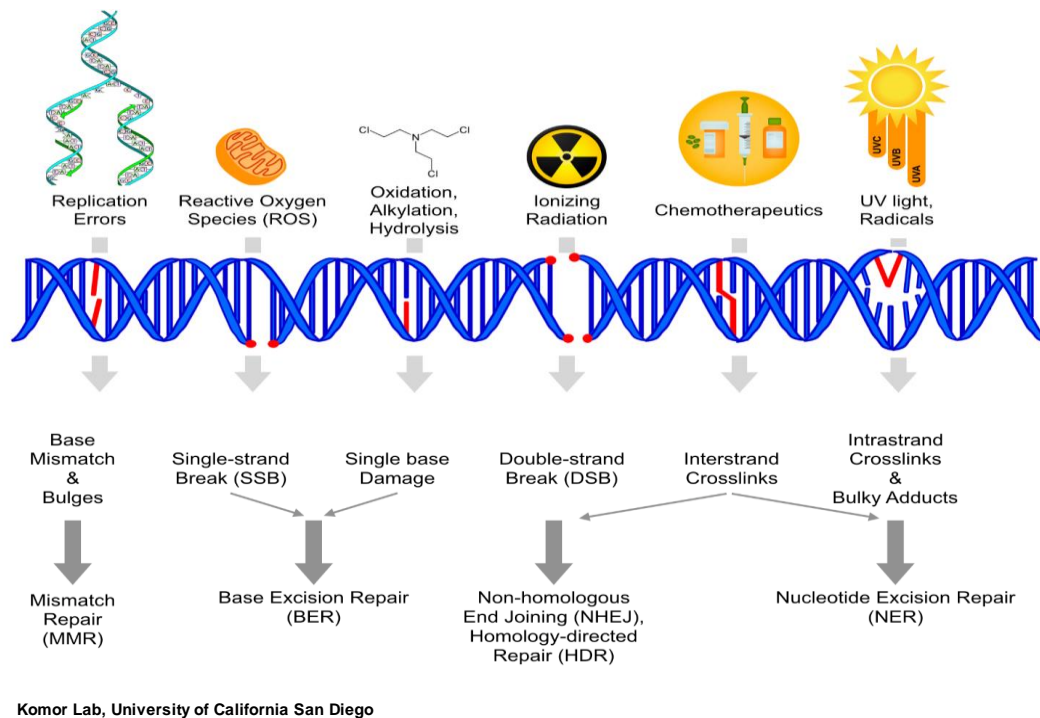


Figure 1 Causes of DNA damage and related repair pathways

Graphical representation of various DNA damage agents such as replication errors, reactive oxygen species, oxidation, ionizing radiation, chemotherapy and UV radicals and the associated DNA repair pathways related to particular type of DNA damage.

Cells employ multiple strategies to repair DNA damage, including base-excision repair (BER), nucleotide excision repair (NER), homologous recombination (HR), and nonhomologous end joining (NHEJ). BER corrects small, non-distorting lesions in DNA, such as removing a damaged base, by utilizing specific DNA glycosylases for recognition and removal. A DNA polymerase then fills the resulting gap, which is sealed by a DNA ligase. NER, on the other hand, addresses larger, helix-distorting lesions caused by sources like ultraviolet light. The damaged DNA is first identified by specific proteins, and then a large fragment of the affected strand is removed. A DNA polymerase fills the gap, and a DNA ligase seals it. HR efficiently and accurately repairs double-strand breaks in DNA by using a homologous DNA molecule as a template. This error-free process can restore the original DNA sequence. NHEJ, in contrast, rapidly fixes DNA double-strand breaks by directly joining the broken ends,

although it is less accurate and may result in the loss or rearrangement of DNA sequences. (Reviewed in Chatterjee and Walker, 2017; Ripley et al., 2020).

The replication of DNA is an essential step for cells before they can divide. It ensures the accurate inheritance of genetic traits. DNA replication occurs during the S phase of the cell cycle. It is a complex and conserved process involving the participation of multiple proteins composed of several dozens of polypeptides, including the CMG (Cdc45/Mcm2-7/GINS) complex, DNA polymerases (Pol α , Pol δ , Pol ϵ), PCNA, Mrc1 (mediator of replication checkpoint 1), Tof1 (topoisomerase 1-associated factor 1), topoisomerases, Okazaki fragment maturation proteins Dna2 and Fen1, and DNA ligase. Okazaki fragments are small, 200-base pieces of the lagging strand of DNA that are produced during replication. Any flaws during DNA replication can result in lethal genomic mutations that can lead to cancer (Branzei and Foiani, 2010). DNA synthesis initiates in the S phase when the replicative helicase unwinds and separates the two strands of DNA. All known DNA polymerases have a 5'→ 3' polymerisation activity, with one strand – the leading strand – of the replicating DNA undergoing continuous synthesis, and the other strand – the lagging strand – undergoing synthesis of short fragments, forming Okazaki fragments (Figure 2).

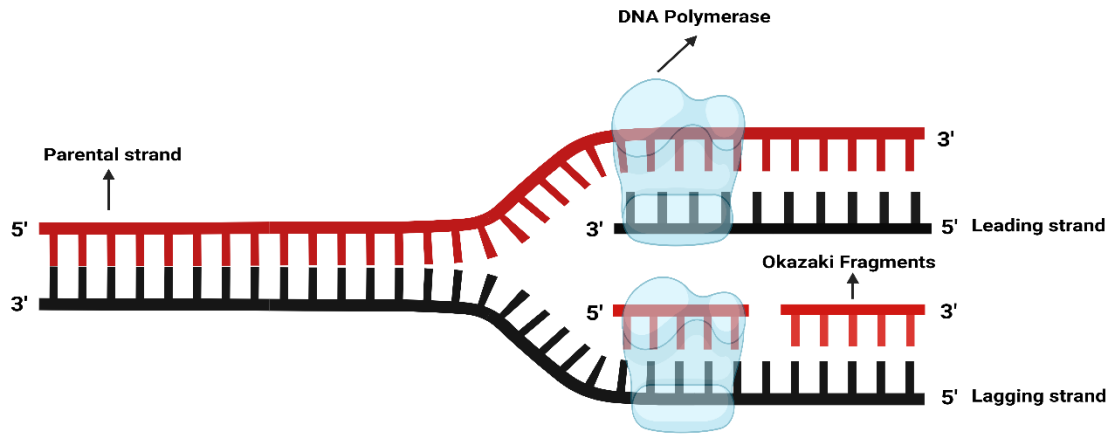


Figure 2 Representation of the DNA replication fork

The eukaryotic replication fork is illustrated in a diagram, where the Okazaki fragments on the lagging strand are depicted as red fragmented strand . DNA Polymerase is shown replicating the leading strand.

Proliferating cell nuclear antigen (PCNA) functions as a “sliding clamp” that encircles the DNA and helps to maintain the fidelity of replication. It does this by stabilising the interaction between the DNA polymerases and the template DNA, allowing for efficient and accurate synthesis. Mrc1, Tof1, and topoisomerases also play important roles in the replication process, with Mrc1 acting as a sensor for replication stress (replication stress refers to a situation in which cells face difficulties in accurately replicating their DNA), Tof1 regulating the activity of the CMG complex (the CMG complex acts as a replicative helicase), and topoisomerases helping to relieve the torsional stress that builds up at the replication fork.

Two processes are responsible for bypassing damaged DNA: translesion synthesis and template switching. TLS is a process in which the DNA polymerase, the enzyme synthesising new DNA strands, can bypass lesions or damaged bases in the DNA template and continue DNA synthesis. This allows the cell to continue replicating its DNA, even in the presence of damage. Template switching is a process that occurs during DNA replication, in which the replication machinery switches from one template strand to the other to continue DNA synthesis. This mechanism ensures that

replication can proceed even if one of the template strands is damaged or unable to serve as a template for DNA synthesis. (Boiteux and Jinks-Robertson, 2013; Friedberg et al., 2002; Marians, 2018).

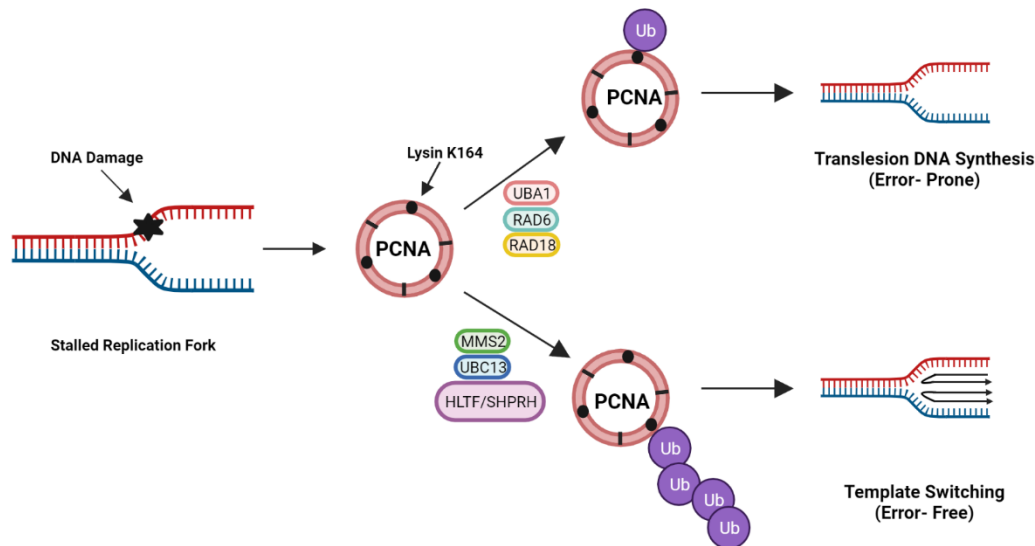


Figure 3 Detailed representation of DNA damage repair pathways at the stalled replication fork

Monoubiquitination of (PCNA) at lysine K164 is triggered by the stalling of the replication fork due to DNA-damaging agents. Monoubiquitinated PCNA activates TLS, an error-prone DNA damage tolerance process. In the presence of Mms2, Ubc13, and HLTf or SPRH, monoubiquitinated PCNA can undergo polyubiquitination, initiating error-free template switching.

Translesion synthesis is accomplished through nucleotide incorporation, utilising the damaged DNA as a template. The development and expansion of the chicken foot intermediate (which occurs when cells are trying to repair broken ends of DNA, often during the process of non-homologous end joining) are required for the template switching pathway (Figure 3).

When the replicative DNA polymerase enzyme encounters a lesion or a damaged base in the DNA template, it is normally unable to synthesise a new DNA strand past this point. However, during TLS, the replicative polymerase is replaced by a

specialised TLS polymerase that is able to bypass the lesion and continue DNA synthesis.

1.2. PCNA

PCNA has been referred to as a “sliding clamp.” The β component of *E. coli* Pol III provided the first evidence for the sliding clamp structure. In a series of elegant experiments, it was demonstrated that the β subunit bonded strongly to nicked circular plasmids but easily detached upon plasmid linearisation via sliding over the ends (Stukenberg et al., 1991; Yao et al., 1996). These findings pointed to a topological binding mode in which the β subunit encircles DNA. Each PCNA protomer is composed of two topologically identical globular domains linked by an interdomain connecting loop (IDCL) (Figure 4. (Dieckman et al., 2012)).

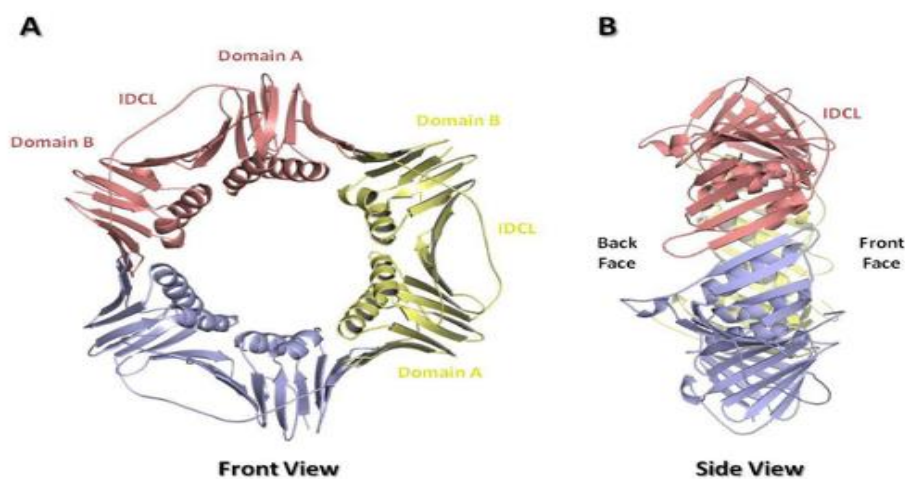


Figure 4 Structure of PCNA

Ribbon diagram of the PCNA trimer (PDB ID:1PLQ) is shown from the front (**A**) and side (**B**) with the individual PCNA subunits coloured red, yellow, and blue. The inter-domain connector loop (IDCL) is indicated (Dieckman et al., 2012).

PCNA also plays an important role in controlling DNA damage tolerance pathways. It is loaded onto DNA with the help of a protein complex known as replication factor C (RFC) (Majka and Burgers, 2004). In response to DNA damage that has not yet been

repaired by other processes, PCNA is ubiquitinated at a specific lysine residue, K164. This results in the replacement of classical polymerases by TLS polymerases to PCNA, making it easier to bypass the lesion and enabling tolerance to DNA damage.

In response to PCNA monoubiquitination, the TLS pathway is activated, and replicative DNA polymerases are switched to TLS polymerases (characterised by relatively non-selective and open active sites and lack of 3'→5' proofreading exonuclease activity) that can replicate across the DNA lesion and are therefore promising targets for cancer chemotherapy (reviewed in (Saha et al., 2021; Vaisman and Woodgate, 2017; Yang and Gao, 2018). Similarly, PCNA can be polyubiquitinated, which sets in motion a separate mechanism of template switching (reviewed in Branzei and Szakal, 2017, 2016). The heterodimeric E2 complex Mms2-Ubc13 and E3 proteins HLTF or SHPRH are involved in the polyubiquitination of PCNA. The polyubiquitin chain forms on ubiquitin's K63 residue instead of K48, the former of which causes template switching, and the latter is recognised and degraded by the proteasome (reviewed in Gallo and Brown, 2019; Kanao and Masutani, 2017; Leung et al., 2018; Ripley et al., 2020; Wilkinson et al., 2020). PCNA is also SUMOylated on Lys164 by Ubc9 (a SUMO-conjugating enzyme) and Siz1 (a SUMO ligase), in addition to monoubiquitination and polyubiquitination (Hoege et al., 2002).

PCNA SUMOylation inhibits undesired recombination by enlisting the anti-recombinogenic Srs2 helicase. The Rad51 nucleoprotein filaments required for the strand exchange reaction are then damaged by the Srs2 helicase. On Lys127 in the IDCL, SUMOylation has also been detected to a lesser extent; however, the biological effects of SUMOylation are unknown (reviewed in Dieckman et al., 2012).

In addition, it has been discovered that other ubiquitin-like proteins, such as neural precursor cell expressed developmentally downregulated 8 (NEDD8) and interferon-stimulated gene 15 (ISG15), are also able to modify the lysine 164 residue of PCNA. Each of these modifications occurs through a different E1-E2-E3 cascade, although there may occasionally be some overlap (Zhang et al., 2021). The precise function of these post-translational modifications is currently not clear, but under oxidative stress, NEDDylation regulates the recruitment of TLS polymerase, and ISGylation regulates the release of TLS polymerases from PCNA complexes, which aids in the termination of TLS (Guan and Zheng, 2019; Hoege et al., 2002; Park et al., 2014).

1.3. The role of Rad6

Ubiquitination regulates a multitude of cellular processes in eukaryotes, such as protein degradation, DNA repair, transcription, protein trafficking, the cell cycle, and vesicle budding. The E2 enzyme is primarily responsible for determining the characteristics of ubiquitin modification, while the E3 ligase often contributes significantly to the process (Komander and Rape, 2012). Although we have a better grasp of the interactions that drive each phase of the ubiquitination cascade thanks to structural studies, our knowledge of how differences between E2 enzymes govern substrate selectivity is still limited (Berndsen and Wolberger, 2014; Schulman and Wade Harper, 2009; Wenzel et al., 2011). There are approximately 35 human E2 enzymes and approximately 12 yeast E2 enzymes, each of which has had varied degrees of polyubiquitinating activity investigated.

The Rad6 protein in the yeast *Saccharomyces cerevisiae* and its human homologues, RAD6A/B, are conserved E2 enzymes that play a crucial role in both transcription and DNA repair processes. Unlike other E2 enzymes, which are unable to modify substrates without the help of an E3, the yeast and human homologues of Rad6 are

capable of doing so on their own. Rad6 has a crucial role in DNA repair by monoubiquitinating PCNA on lysine 164 in a process mediated by the Rad18 E3 ligase (Figure 5A). Monoubiquitination of PCNA is important for the recruitment of translesion synthesis polymerases, which are responsible for replicating DNA across damaged or blocked replication forks, this process is known as translesion synthesis-dependent DNA repair. Rad6 possesses an innate ability to create polyubiquitin chains, but this ability is suppressed when it associates with Rad18, allowing for the attachment of just a single ubiquitin molecule to PCNA (Bailly et al., 1994). Together with the E3 ligase Bre1, Rad6 is responsible for the modification known as monoubiquitination of histone H2B at position K123 (Figure 5B). This modification is critical for transcriptional activation and elongation, in addition to DNA splicing (Hwang et al., 2003; Robzyk et al., 2000; Wood et al., 2003).

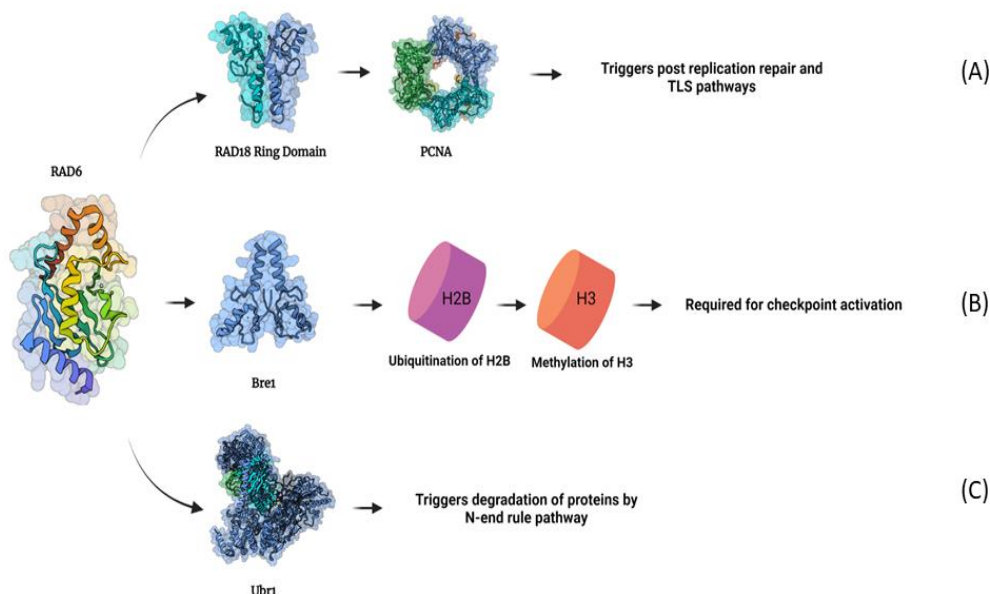


Figure 5 Schematic representation of Rad6 and its different roles

(A) Rad6 interaction with E3 ligase Rad18 triggers the monoubiquitination of PCNA. **(B)** Rad6 also plays a role in histone ubiquitination by interacting with Bre1. **(C)** It also facilitates the proteasomal degradation of substrates through the N-end rule pathway.

Through the N-end rule pathway, yeast Rad6 and the E3 ligase known as Ubr1 also play a role in the proteasomal degradation of substrates by binding K48-linked polyubiquitin to the substrates (Figure 5C). The N-end rule pathway is a protein degradation system that recognizes proteins with destabilizing N-terminal residues and targets them for degradation by the proteasome. The pathway is conserved from bacteria to mammals and plays an important role in regulating a variety of cellular processes, including cell cycle progression, DNA damage repair, and response to stress (Sriram et al., 2011).

2. Goals and Objectives

The study aimed to develop and optimise high-throughput *in vitro* assays to investigate the PCNA ubiquitination cascade and screen for small molecule modulators PCNA ubiquitination. Monoubiquitination of PCNA triggers the TLS pathway, where replicative DNA polymerases are substituted with more error-prone TLS polymerases that can replicate across DNA lesions. By targeting the PCNA ubiquitination cascade using small molecule inhibitors, either alone or in combination, we could potentially hinder cancer progression.

Experimental approach:

- Developing and optimising highly sensitive and reliable assays for the PCNA ubiquitination cascade based on amplified luminescent proximity homogeneous assay (Alpha) technology.
- Performing the screening of chemical libraries to discover modulators of the PCNA ubiquitination reaction.
- Characterising the hits from the primary screening to determine the target.

3. Materials and Methods

3.1. FLAG-PCNA

The pBJ842 yeast expression vector was used to clone Human GST-Flag tagged PCNA. The *S. cerevisiae* BJ5654 strain was utilized for the expression, and affinity chromatography was employed with glutathione beads for purification. The cells were washed in 1× phosphate-buffered saline (PBS), then dropped into liquid nitrogen, and ground with a SPEX SamplePrep 6775 Freezer/Mill. The lysate underwent centrifugation, and the supernatant was applied to a glutathione agarose (Machery-Nagel) column with the GST tag being cleaved by a precision protease. The concentration was determined by measuring the absorbance at 280 nm using a NanoDrop ND 100 spectrophotometer and calculating the concentration of all proteins using the ProtParam tool with the extinction coefficient of proteins followed by the Beer-Lambert Law.

3.2. GST-Flag-Uba1

Human Flag-tagged Uba1 was introduced into the pBJ842 yeast expression vector with the Leu marker followed by expression in *S. cerevisiae* BJ5654 strain and purification with cleavage of the GST moiety, as mentioned in section 3.1.

3.3. FLAG-Ubr1

FLAG-Ubr1 Addgene (#24506) was introduced into the pBJ842 yeast expression vector. The *S. cerevisiae* BJ5654 strain was used for the expression, followed by purification and elution using Flag-peptide.

3.4. FLAG- Rad6, FLAG-Rad18, FLAG-UBC13 and FLAG-MMS2

The Gateway cloning technology (Life Technologies) was used to create constructs. The cDNA sequences of human Rad6B, human Rad18, UBC13, and MMS2 from the entry constructs were combined with a modified pGEX-6P-1 (Amersham) destination vector that had GST and FLAG tags and a Gateway cassette, through the LR Clonase II reaction (Invitrogen). *E. coli* strain BL21-CodonPlus (DE3)-RIL (Agilent) was used to overexpress the proteins, which were later purified by removing the GST moiety, as described above. as mentioned in section 3.1.

3.5. GFP-Rad6 and GFP-Rad18

Constructs were generated with Gateway cloning technology (Life Technologies). Human GFP-Rad6B and human GFP-Rad18 cDNA sequences from entry constructs were recombined into a modified pGEX-6P-1 (Amersham) destination vector bearing GST and GFP tags with a Gateway cassette via the LR Clonase II reaction (Invitrogen). Proteins were overexpressed in the *E. coli* strain BL21-CodonPlus (DE3)-RIL (Agilent). The proteins were purified with the removal of the GST moiety, as mentioned in section 3.1.

3.6. Rad6-Rad18 dimer

Both human Rad6B and GST-fused human Rad18 constructs (each cloned into the pBJ842 yeast expression vector, containing Leu and Trp auxotrophic markers) were introduced into the *S. cerevisiae* BJ5654 strain. The cells were grown in omission media (–Leu, –Trp), then collected when reaching OD₆₀₀ 0.8–1, centrifuged, and washed with 1× PBS. The cells were resuspended in yeast lysis buffer consisting of 50 mM HEPES, pH 7.5, 50 mM KCl, 267 mM NaCl, 10% sucrose, 0.5 mM EDTA, and 2.8 mM β-mercaptoethanol. The cell lysate was then dropped into liquid nitrogen, ground with a SPEX SamplePrep 6775 Freezer/Mill, collected into 1.5 ml

microcentrifuge tubes, and centrifuged. The supernatant was applied to a glutathione Sepharose 4B (GE Healthcare) column, followed by repeated washings in 20 mM Tris-HCl, pH 7.5, 10% glycerol, 0.01% NP-40, and 1 mM DTT at progressively lower NaCl concentrations (3× 500 mM, 3× 250 mM, 1× 150 mM). The GST moiety was cleaved with PreScission Protease (GE Healthcare) with incubation for 2 h at 4°C with light shaking, and the dimer was eluted with a 1.5× bed volume equivalent of 20 mM Tris-HCl, pH 7.5, 150 mM NaCl, 10% glycerol, 0.01% NP-40, and 1 mM DTT.

3.7. GST-Ubiquitin

Human GST-tagged ubiquitin was expressed in the *E. coli* strain Dh5α. The bacterial culture was grown in LB medium overnight in the presence of ampicillin at 37°C with continuous shaking. The cells were induced with 200 μM IPTG for 5 h at 18°C. The cells were centrifuged and washed in 1× phosphate-buffered saline (PBS), followed by sonication. The cell lysate was then centrifuged, and the supernatant was applied to a glutathione-Sepharose 4B beads (Machery-Nagel) column. The protein was eluted from the column using 20 mM reduced glutathione after repeated washing.

3.8. His-Uba1

His-tagged human Uba1 in the pET3a bacterial expression vector (Addgene plasmid #63571, courtesy of Titia Sixma) was expressed in *Escherichia coli* strain BL21-CodonPlus (DE3)-RIL (Agilent). The cells were centrifuged and washed in 1× phosphate-buffered saline (PBS), followed by sonication. The cell lysate was then centrifuged, and the supernatant was applied to a Ni-nitrilotriacetic acid (NTA) agarose (Machery-Nagel) column. Following repeated washings, the protein was eluted from the column with 250 mM imidazole, then dialysed against 20 mM Tris-HCl, pH 7.5, 150 mM NaCl, 10% glycerol, 0.01% NP-40, and 1 mM freshly added dithiothreitol (DTT). The concentration was determined as mentioned in section 3.1.

3.9. RFC complex

The construct pLANT-2/RIL–RFC [1s +5] was co-transformed with the construct pET(11a)–RFC [2+3+4] (Finkelstein et al. 2003) into the *E. coli* strain BL21-CodonPlus(DE3)-RIL (Agilent), where RFC1s represents an N-terminally truncated form of the large RFC subunit (Gomes and Burgers 2000). The cells were plated and allowed to grow under selection with ampicillin (100 µg/ml) and kanamycin (50 µg/ml) overnight. A single transformant colony was then picked and grown in 2 ml of Luria-Bertani medium containing ampicillin (100 µg/ml) and kanamycin (50 µg/ml) at 37°C for 8 h, then inoculated into a starter culture of 2 l of Luria-Bertani medium containing ampicillin (100 µg/ml) and kanamycin (50 µg/ml) for 16 h. 300 ml of the starter culture was inoculated into 2 l of Luria-Bertani medium and grown to OD₆₀₀ 0.8 at 37°C. The cultures were cooled to 16°C and induced with 0.5 mM isopropyl-β-D-thiogalactoside for 16 h. All further steps were performed at 4°C. The cells were harvested by centrifugation and then resuspended in HEG buffer (30 mM HEPES, pH 7.6, 0.5 mM EDTA, 10% glycerol, 5 mM β-mercaptoethanol) containing 150 mM NaCl. To lyse the cells, lysozyme was added to 0.4 mg/ml, and the cells were subjected to three freeze-thaw cycles, followed by mechanical shearing through a hypodermic needle. The cell lysate was treated with Benzonase endonuclease, purity grade II (Merck), according to the manufacturer's protocol. The cell lysate was clarified by centrifugation. RFC was purified by chromatography over an SP-Sepharose column (bed volume of 6 ml), pre-equilibrated with HEG with 50 mM NaCl, followed by a wash with 60 ml of HEG buffer containing 50 mM NaCl. Elution was carried out with a gradient of 50–1,000 mM NaCl in a 60 ml HEG buffer. Peak fractions were collected, pooled, and then diluted with NiNTA buffer (30 mM HEPES, pH 7.6, 20 mM imidazole, 500 mM NaCl, 10% glycerol, 5 mM β-mercaptoethanol). The resulting sample was then applied to a NiNTA agarose

(Machery-Nagel) column (bed volume of 500 μ l), pre-equilibrated with NiNTA buffer. The column was then washed with 5 ml of Ni-NTA buffer, and proteins were eluted by a three-step gradient (100 mM, 250 mM, and 500 mM imidazole), each with 1.5 ml overall volume. Fractions were tested for PCNA loading ability, and peak fractions were aliquoted, frozen in liquid N₂, and stored at -80°C until subsequent use.

3.10. Plasmids, antibodies, and other reagents

Dh5 α cells were transformed with pUC19 plasmid and the cells were cultured for 16 hours at 37°C. The plasmid was purified using the Qiagen QIAprep Spin Miniprep Kit after collecting the cells via centrifugation. Nt. BstNBI enzyme was used to nick the plasmid overnight at 50°C, and the agarose gel electrophoresis technique was employed to verify the digestion. Biotinylated human ubiquitin was obtained from Boston Biochemicals/R&D Systems, while Streptavidin donor and anti-FLAG acceptor AlphaLisa and AlphaScreen beads were purchased from PerkinElmer. HRP-conjugated anti-FLAG M2 monoclonal antibody was purchased from Sigma-Aldrich, and anti-GST HRP-conjugated antibody from GE Healthcare. Santa Cruz Biotechnology provided anti-DNA polymerase delta catalytic subunit and anti-tubulin antibody. PreScission Protease was used as required to digest GST-tagged proteins, and the NCI provided the chemical library.

3.11. Alpha assays

We obtained Alpha beads from PerkinElmer for the purpose of conducting Alpha assays, which employ the luminescent oxygen channelling immunoassay and have been licensed to PerkinElmer. There are two varieties of the Alpha assay, AlphaScreen, and AlphaLISA, both of which rely on excitation at 680 nm. The only difference between them lies in the fluorophores utilized in the acceptor beads.

AlphaScreen utilizes anthracene and rubrene, which have an emission maximum of 520-620 nm, while AlphaLISA utilizes a europium chelate, which has an emission maximum of 615 nm. The donor beads, however, remain the same in both assays. For our experiments, we employed AlphaScreen acceptor beads. The donor beads were coated with streptavidin, unless otherwise stated, while the acceptor beads were coated with anti-FLAG antibodies. The plates used for both screening and follow-up Alpha experiments were examined using a Tecan Spark plate reader equipped with a laser dedicated to Alpha assays, a plate stacker, and a temperature control module to regulate temperature precisely. All Alpha assays were performed using 96-well white round-bottom polypropylene plates (Greiner) at a temperature of 25°C, unless otherwise noted.

3.12. PCNA ubiquitination

PCNA ubiquitination reactions were performed in 96-well white round-bottom polypropylene plates (Greiner) with 150 nM biotinylated ubiquitin, 50 nM FLAG-PCNA, 2 nM RFC, 2 nM nicked pUC19 plasmid DNA, 50 nM Uba1, and 100 nM Rad6–Rad18 complex in the reaction buffer consisting of 40 mM Tris-HCl, pH 7.5, 8 mM MgCl₂, and 10% glycerol (Reaction Buffer). The reactions were preincubated with compounds for 15 min, followed by initiation by adding 100 μM ATP and incubation for 2 h at 25°C. The final volume of each reaction was 20 μl here and in the experiments described below. Reactions were terminated by 10x dilution with a buffer we designate Alpha Buffer consisting of streptavidin donor and anti-FLAG acceptor AlphaScreen beads (10 μg/ml), 25 mM HEPES, pH 7.5, 100 mM NaCl, 0.1% Tween 20, 20 mM ethylenediaminetetraacetic acid (EDTA), and 1 mM dithiothreitol (DTT). The samples were incubated in the dark at 25°C for 4 h and then read in a Tecan plate reader.

3.13. Uba1~ubiquitin thioester formation

The reactions were performed with 50 nM FLAG-Uba1 and 150 nM Biotin-ubiquitin in Reaction Buffer. Compounds were added separately, and samples were incubated for 15 min at 25°C. Initiation of the reactions was carried out by the addition of 100 µM ATP, then incubated for 30 min at 25°C, followed by stopping and dilution by a factor of 10x in Alpha Buffer (no DTT was added so as to not cleave the thioester), with donor and acceptor beads at 10 µg/ml. The samples were incubated, and the plates were read by a Tecan plate reader.

3.14. Rad6~ubiquitin thioester formation

For the first step of Uba1 pre-charging, 100 nM His-Uba1 and 300 nM biotin ubiquitin were incubated with 100 µM for 30 min at 25°C. Then compounds were incubated with 100 nM Flag-Rad6 for 15 min. Both reactions were mixed and incubated for 30 min at 25°C, followed by termination and dilution by a factor of 10x in Alpha Buffer (without DTT), with donor and acceptor beads at 10 µg/ml. Then the samples were incubated in the dark for 4 hours, and the plates were read as above.

3.15. Rad18 autoubiquitination

His-Uba1 (50 nM) was pre-charged with biotinylated ubiquitin (100 nM) by adding 100 µM ATP in Reaction Buffer, followed by incubation for 30 min. Then FLAG-Rad18 (100 nM), Rad6–Rad18 complex (100 nM, with Rad6–Rad18 prepared as a coexpressed complex in yeast, according to published procedures (Fenteany et al., 2020)) were incubated with compounds for 15 min. Both reactions were mixed and incubated for an additional 1 h at 25 °C, followed by termination and dilution by a factor of 10x in Alpha Buffer, with donor and acceptor beads at 10 µg/ml. The samples were incubated, and the plates read as above.

3.16. Rad6–Rad18 interaction

The reaction was performed using 100 nM of Flag-Rad6 and 100 nM of His-Rad18, which were pre-incubated together for 30 minutes in a reaction buffer to form a complex. After the complex was formed, the compound was added to the mixture, and the sample was incubated for an additional 15 minutes at 25°C. The samples were diluted by a factor of 10× in Alpha Buffer, with donor and acceptor beads at 10 µg/ml. The samples were incubated, and the plates read as mentioned above.

3.17. Mms2–Ubc13~ubiquitin thioester formation

For the first step of Uba1 pre-charging, 100 nM Flag-Uba1 and one µM GST-ubiquitin were incubated with 100 µM ATP for 30 min at 25°C. Then compounds were incubated with one µM Mms2–Ubc13 for 15 min. Both reactions were mixed and incubated for 30 min at 25°C. Detection was performed by silver staining.

3.18. Microscale thermophoresis

Microscale thermophoresis was performed to observe the small molecule–protein binding using a NanoTemper Monolith instrument. The compound was serially diluted 16 times, starting with 4 mM by factors of two (4 mM – 122.07 nM), and incubated with 20 nM of green fluorescent protein (GFP)-Rad6 or GFP-Rad18 for 15 min. Sixteen capillaries were then filled with each dilution, loaded into the NanoTemper Monolith instrument, and the native software was used to determine the K_d (K_D, or dissociation constant, is a measure of the strength of binding between two molecules, typically a protein and a ligand. It is defined as the concentration of ligand at which half of the protein binding sites are occupied by the ligand) from the titration data.

3.19. Rad6–Ubr1 pull-down

Equimolar GST-Rad6 and FLAG-Ubr1 (1 μ M) were mixed and incubated with the compound (NSC 9037) for 15 min at 25°C and then loaded onto an affinity chromatography column containing glutathione-agarose beads. Elution was done with 20 mM glutathione and visualisation by silver staining.

3.20. Rad6–Ubr1 interaction alpha assay

Equimolar GST-Rad6 and FLAG-Ubr1 (100 nM) were mixed and incubated with the xanthene compounds for 15 min at 25°C in reaction buffer, followed by dilution by a factor of 10 \times in Alpha buffer, with donor and acceptor beads at 10 μ g/ml. After 4-h incubation at 25°C in the dark, the plates were read by the plate reader.

3.21. Cell culture

HeLa cells were cultured in a growth medium consisting of Dulbecco's modified Eagle's medium (DMEM from Sigma-Aldrich) with 10% fetal bovine serum (FBS from Gibco) in a humidified cell culture incubator at 37°C with 5% CO₂.

3.22. Cell survival

A 96-well cell culture plate was used to culture HeLa cells at a density of 1 \times 10⁴ cells in 50 μ l per well. The culture medium used was DMEM containing 0.5% FBS, and the cells were incubated at 37°C and 5% CO₂. After 24 hours, the compounds, or DMSO alone, were added to the wells. The cells were treated with the compounds for another 24 hours, and then resazurin (Alamar Blue) was added. 4 hours later, the plate was analyzed on a fluorescence plate reader with excitation at 570 nm and emission at 585 nm to measure the change in color.

3.23. Computational docking of compounds to Rad6

The nuclear magnetic resonance solution structure of the full-length human Rad6B (PDB ID: 2Y4W) (Huang et al., 2011) was retrieved from the Research Center for Structural Genomics Protein Data Bank. The ten lowest energy structures were published as targets for docking. We utilised the Autodock 4.2 software and the Lamarckian genetic algorithm with default parameters to perform parallel, blind dockings of the Rad6B protein. The maximum number of energy evaluations was set to 2,500,000, and the dockings were carried out in two grid volumes measuring 90.0 Å x 124.0 Å x 90.0 Å, covering the entire surface of the protein. The grid spacing was set to 0.375 Å, and all ligand torsions were kept flexible during the dockings. While the protein coordinates were kept rigid, the internal flexibility of the protein was partially accounted for by docking to 10 different structural states. A total of 1,000 dockings were performed for each target and grid, resulting in an ensemble of 20,000 Rad6–NSC 9037 complexes.

These complexes were then clustered using a tolerance of 2.0 Å and ranked according to the corresponding binding free energies. *In silico* inhibitory constants were calculated from binding free energies derived from docking, according to the following equation: $\Delta G = RT \ln K_i$. Selected high-affinity binding poses were subjected to further contact analysis. The selection of potential binding poses was based on their predicted binding affinities and apparent site specificity and omitted low-affinity surface-bound poses; then, we selected 4-14 high-affinity binding poses for each of the 10 Rad6B structural states and subjected them to further contact analysis. We also performed a second series of refined flexible blind dockings using a single Rad6 target structure that was selected based on pilot blind dockings and extended this to include all of the compounds. Furthermore, amino acid side chains which were found in the pilot

dockings to participate in protein-ligand interactions frequently were kept flexible in the second series (Table 2.), providing 18–32 torsional degrees of freedom during the respective dockings. All other docking parameters were the same as above. K_i values were derived from the binding free energies, and specific residues of contact were determined for these refined binding poses

3.24. QUANTIFICATION AND STATISTICAL ANALYSIS

GraphPad Prism 8 and Microsoft Excel were used to calculate all the IC₅₀ (the concentration of a drug or other compound that is required to inhibit half of the maximum response of a biological system).and curve fitting calculations. Statistical parameters used for the analysis:

Signal-to-noise (S/N) and Signal-to-background (S/B) = They are indication of the degree of confidence with which a signal can be regarded as real.

$$S/N = \frac{\text{mean signal} - \text{mean background}}{\text{standard deviation of background}}$$

$$S/B = \frac{\text{mean signal}}{\text{mean background}}$$

z-factor: The z-factor is defined in terms of four parameters: the mean and standard deviation of both positive and negative controls.

$$Z = 1 - \frac{3SD \text{ of sample} + 3SD \text{ of control}}{\text{mean of sample} - \text{mean of control}}$$

Strictly standardised mean difference (SSMD) and Signal window values: It is the mean divided by the standard deviation of the difference between two random groups. On the other hand, the signal window value is a more indicative measure of the data range in the HTS assay.

Statistical details can be found in the figure legends.

4. Results and conclusion

4.1. Development and optimisation of ALPHA-based PCNA ubiquitination assay for high-throughput screening.

We have developed and optimised an *in vitro* ALPHA-based (amplified luminescent proximity homogeneous) assay for PCNA ubiquitination to discover small molecule inhibitors (Fenteany et al., 2020). The Alpha system of PerkinElmer operates based on a luminescent oxygen channeling immunoassay, which is a homogeneous bead-based method of immunoassay. The method involves high-energy illumination at 680 nm on the Alpha donor beads, which contains a photosensitizer named phthalocyanine. The irradiation leads to the excitation of the phthalocyanine, transforming the ambient oxygen into a singlet state that is different from the highly reactive superoxide radical. The singlet state of oxygen has a lifespan of around 4 microseconds in aqueous solutions and can diffuse to a distance of approximately 200 nm. If an Alpha acceptor bead is present within this distance, the singlet oxygen can interact with a thioxene derivative in the acceptor bead and generate a chemiluminescent emission that excites fluors present in the acceptor beads (anthracene and rubrene for the AlphaScreen version or a europium chelate for the AlphaLISA version). This produces fluorescent emissions in the range of 520-620 nm (for AlphaScreen) or 615 nm (for AlphaLISA), which are then detected by a photomultiplier tube. We have also developed and optimised *in vitro* ALPHA-based assays for the intermediary steps involved in the process (Uba1-ubiquitin thioester, Rad6-ubiquitin thioester, Rad6- Rad18 interaction, and Rad18 auto-ubiquitination) (Fenteany et al., 2020).

The ubiquitination of PCNA plays a critical role in DNA replication and repair (Slade, 2018). Our assay is quantitative and yields a wide dynamic range with a high signal-

to-noise ratio. We have also confirmed the optimised condition by western blot analysis (Figure 6).

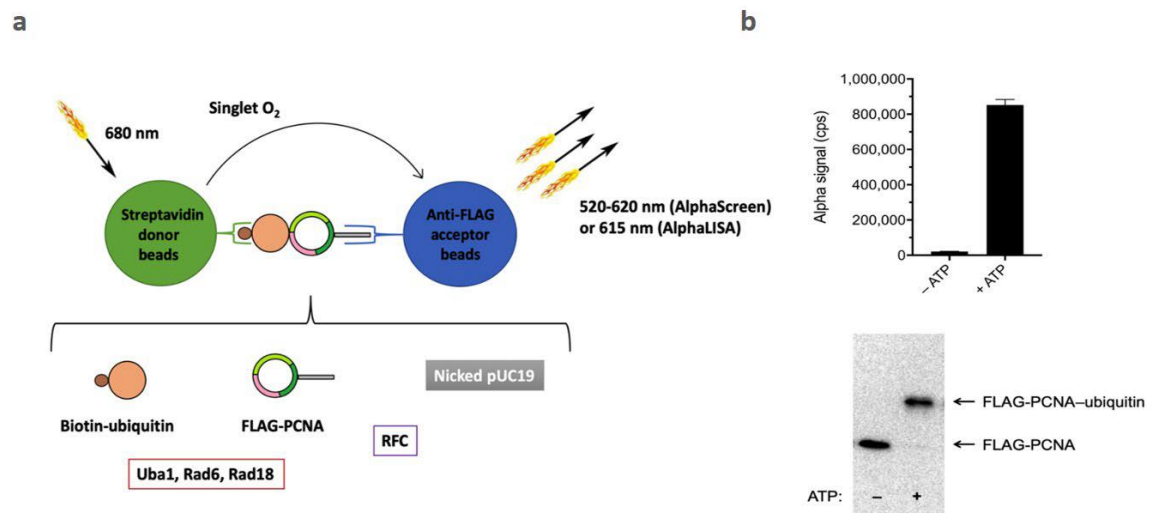


Figure 6 Reconstituted assay for PCNA monoubiquitination.

A. AlphaScreen/AlphaLISA-based high-throughput screening method for *in vitro* PCNA ubiquitination. **B.** PCNA ubiquitination is quantitatively assessed by the Alpha system for both negative (-ATP) and positive (+ATP) ubiquitination reaction cascades. **Lower panel:** Western blot probed with anti-FLAG antibody of samples treated for 2 h without or with ATP reveals non-ubiquitinated FLAG-PCNA (lower band) and ubiquitinated FLAG-PCNA (upper band) (Fenteany et al., 2019).

4.2. Development and optimisation of Rad6–Rad18 interaction assay

We developed a Rad6–Rad18 interaction assay based on the Alpha system to find the small molecules that disrupt or inhibit this interaction (Figure 7). We varied the concentration of each of the two proteins separately, while holding the concentration of the other constant and found satisfactory results over a range of concentrations. We decided to use 100 nM of each protein. Higher concentration of Rad6–Rad18 yielded lower signals which is caused by the occurrence of the high-dose hook effect (excessive analyte concentrations attenuate signals in bimolecular detection assays).

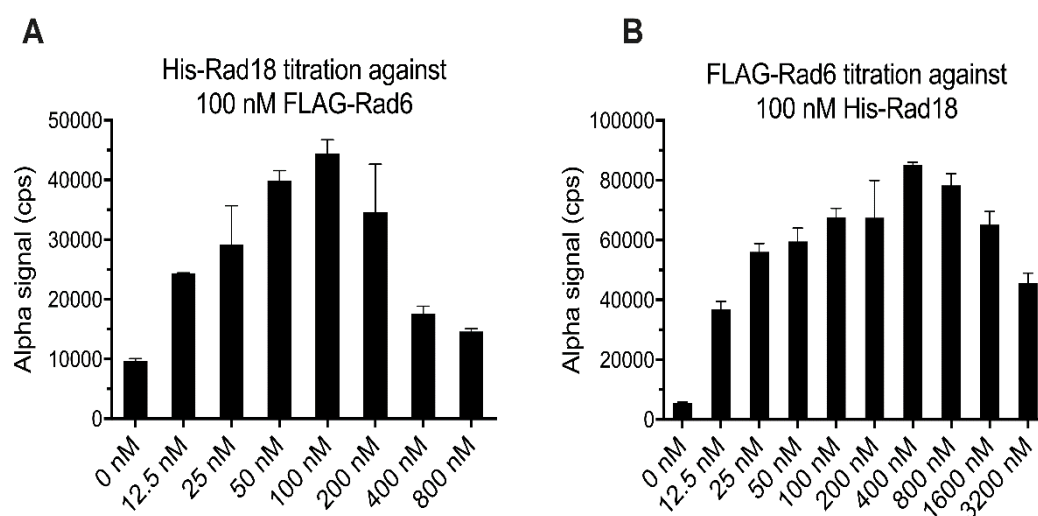


Figure 7 Development of an Alpha assay for the Rad6–Rad18 interaction

(A) Titration of His-Rad18 against FLAG-Rad6. His-Rad18 concentrations were varied as indicated, while FLAG-Rad6 was held constant at 100 nM. **(B)** Titration of FLAG-Rad6 against His-Rad18. FLAG-Rad6 concentrations were varied as indicated, while His-Rad18 was held constant at 100 nM. Data represent the mean with SD (standard deviation) for triplicate samples in each case.

4.3. Screening for inhibitors of PCNA ubiquitination

Compounds blocking PCNA ubiquitination were found using a Microsoft Excel spreadsheet we created, in which we uploaded the data output from the plate reader and automatically generated plate quality control and hit quality criteria. The plate quality control parameters calculated included signal-to-background ratio, signal-to-

noise ratio, signal window, Z' factor in both standard and robust statistical forms (calculated from positive and negative means and medians, respectively), and plate-quality strictly standardised mean difference for plate-quality assessment, both standard and robust. We typically evaluated compounds in triplicates on three independent plates, and if a plate was of low quality according to the estimated metrics, additional plates were screened until there were at least three of acceptable quality (i.e., Z' factors greater than 0.5).

Hit-selection parameters automatically calculated from our spreadsheets included percent normalised change in signal (experimental signal minus the mean of positive signal, with the difference divided by the mean of positive control minus the mean of negative signal), Student's t-tests (in the case of replicate samples, which we typically conduct), z scores (in the case of experiments without replicate samples), and strictly standardised mean differences for hit selection, in both standard and robust formulations. If a compound at a high screening concentration had significant activity, it was then tested at progressively lower concentrations in serial twofold dilutions, with the most active compounds selected with each concentration round. The highest concentration for screening was 10 μ M or 100 μ M depending on stock compound plate concentration (for instance, 1 mM for the NCI DTP Mechanistic Sets and 10 mM for the NCI DTP Diversity Set) that would not exceed 1% dimethyl sulfoxide (DMSO) carrier solvent, the highest concentration of DMSO that did not affect the reaction or the Alpha detection (Fenteany et al., 2020).

4.4. Certain xanthenes and a related acridine derivative inhibit PCNA ubiquitination

We developed and optimised high-throughput assays for screening small-molecule modulators targeting PCNA ubiquitination. Our assays are reconstituted from all the necessary and sufficient elements for PCNA ubiquitination *in vitro*. The method is based on the “amplified luminescent proximity homogeneous assay” (Alpha) system. We screened multiple libraries, including the NCI DTP Diversity Set VI and Mechanistic Set IV. We discovered that one of the compound classes strongly inhibits overall PCNA ubiquitination and is comprised of certain xanthenes and a related acridine derivative (Figure 8). The inhibitory effects of the compounds from the ALPHA assay for overall PCNA ubiquitination and discrete steps in the cascade were confirmed by western blot or gel-based analyses, which showed parallel results (Figures S1, S2, and S3).

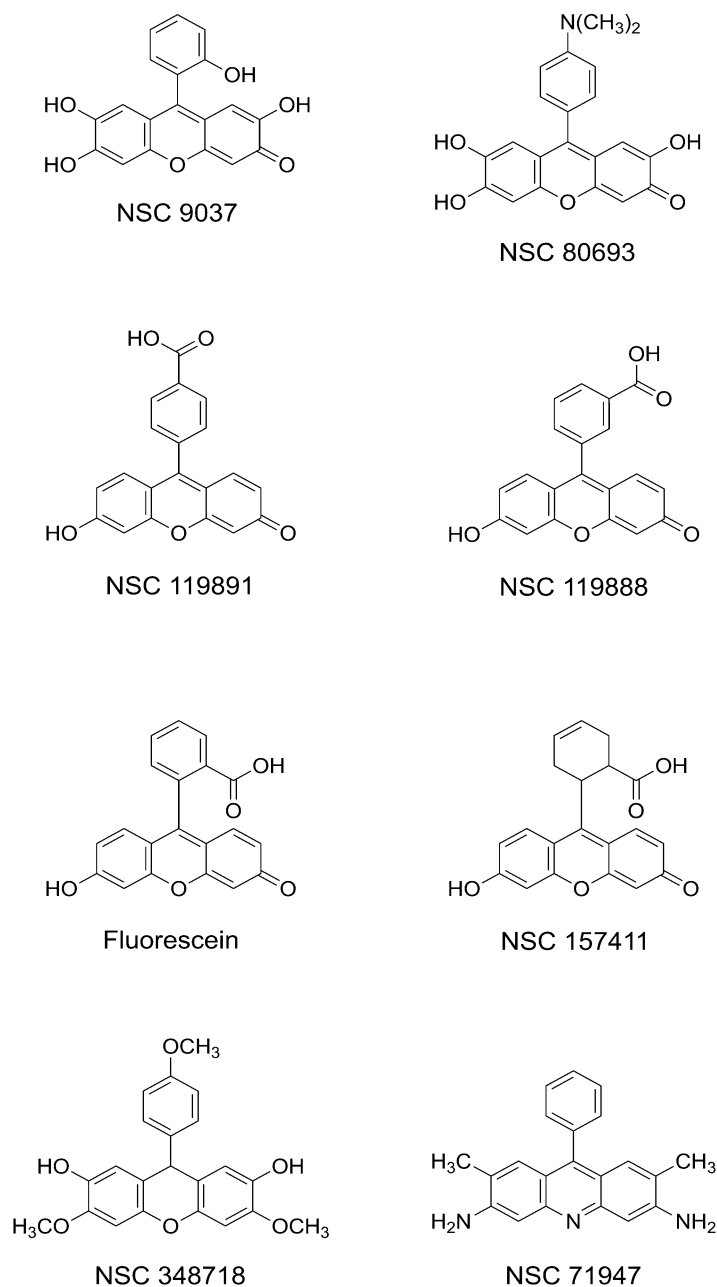


Figure 8 Structures of compounds investigated in this study.

Chemical structure depiction of Xanthenes and a derivative of Acridine (NSC 71947), also including Fluorescein.

4.5. Dose-response analysis for different compounds in PCNA ubiquitination

The dose-response analysis was carried out for PCNA ubiquitination with all eight compounds to get the IC₅₀ for each compound (Table 1) using ALPHA assay as described in Fenteany et al., 2020.

Compound (NSC number)								IC ₅₀ (μM) for cell survival
	PCNA~Ub	Uba1~Ub	Rad6~Ub	Rad18~Ub	Rad6~Rad18	Rad6~Ubr1	Mms2~Ubc13~Ub	
9037	4.543 (SE: 0.9600; CI: 2.607–5.208)	> 100	8.901 (SE: 3.050; CI: 3.945–20.97)	4.460 (SE: 1.071; CI: 2.582–7.698)	6.193 (SE: 0.8657; CI: 4.687–8.194)	> 50	No inhibition on gel at 100 μM	62.23 (SE: 9.861; CI: 44.86–88.31)
80693	4.278 (SE: 0.4380; CI: 3.749–5.623)	> 100	91.84 (SE: 27.7; CI: 60.67–214–)	13.22 (SE: 4.839; CI: 6.589–27.20)	14.58 (SE: 2.341; CI: 11.25–27.10)	Minimal inhibition by Alpha at 50 μM	No inhibition on gel at 100 μM	7.668 (SE: 4.345; CI: 0.5773–23.10)
119891	73.5 (SE: 25.26; CI: 41.14–140.0)	> 100	> 100	> 100	> 100	Minimal inhibition by Alpha at 50 μM	No inhibition on gel at 100 μM	207.5 (SE: 29.38; CI: 170.0–304.2)
119888	56.5.6 (SE: 27.57; CI: 27.57–19.33–)	53.83 (SE: 19.96; CI: 26.10–139.1)	1.903 (SE: 4.087; CI: 1.205–3.094)	>100	> 100	No inhibition by Alpha at 50 μM	No inhibition on gel at 100 μM	75.31 (SE: 10.98; CI: 63.05–89.45)
Fluorescein	> 100	> 100	> 100	> 100	> 100	Minimal inhibition by Alpha at 50 μM	No inhibition on gel at 100 μM	> 100
157411	8.439 (SE: 2.645; CI: 4.411–16.95)	24.82 (SE: 2.556; CI: 20.18–30.57)	22.53 (SE: 3.512; CI: 16.63–40.25)	49.07 (SE: 7.231; CI: 32.27–Ind)	64.71 (SE: 19.34; CI: 40.85–360.3)	No inhibition by Alpha at 50 μM	No inhibition on gel at 100 μM	427.8 (SE: 94.90; CI: 273.9–719.9)
348718	> 100	> 100	> 100	> 100	> 100	No inhibition by Alpha at 50 μM	No inhibition on gel at 100 μM	27.74 (SE: 7.404; CI: 24.56–31.35)
71947	24.89 (SE: 6.218; CI: 15.48–40.26)	> 100	28.33 (SE: 7.496; CI: 16.94–47.38–)	> 100	> 100	Minimal inhibition by Alpha at 50 μM	No inhibition on gel at 100 μM	11.78 (SE: 2.910; CI: 7.199–18.27)

Table 1 Half-maximal inhibitory concentration (IC₅₀) values by Alpha assays for PCNA ubiquitination, Uba1~ubiquitin thioester formation, Rad6~ubiquitin thioester formation, Rad18 autoubiquitination, Rad6~Rad18 interaction, and Mms2~Ubc13~ubiquitin thioester formation.

Included are IC₅₀ values for cell survival. All IC₅₀ values, standard errors, and 95% confidence intervals listed were calculated by nonlinear regression with the GraphPad Prism 8 software. Ub = ubiquitin; SE = standard error; CI = 95% confidence interval; Ind = indeterminate.

We found that a number of the xanthene-3-ones tested – NSC 9037, NSC 80693, NSC 157411, and NSC 119888, as well as the acridine NSC 71947 – inhibited PCNA ubiquitination, while NSC 119891 showed only weak inhibition (Figure 9).

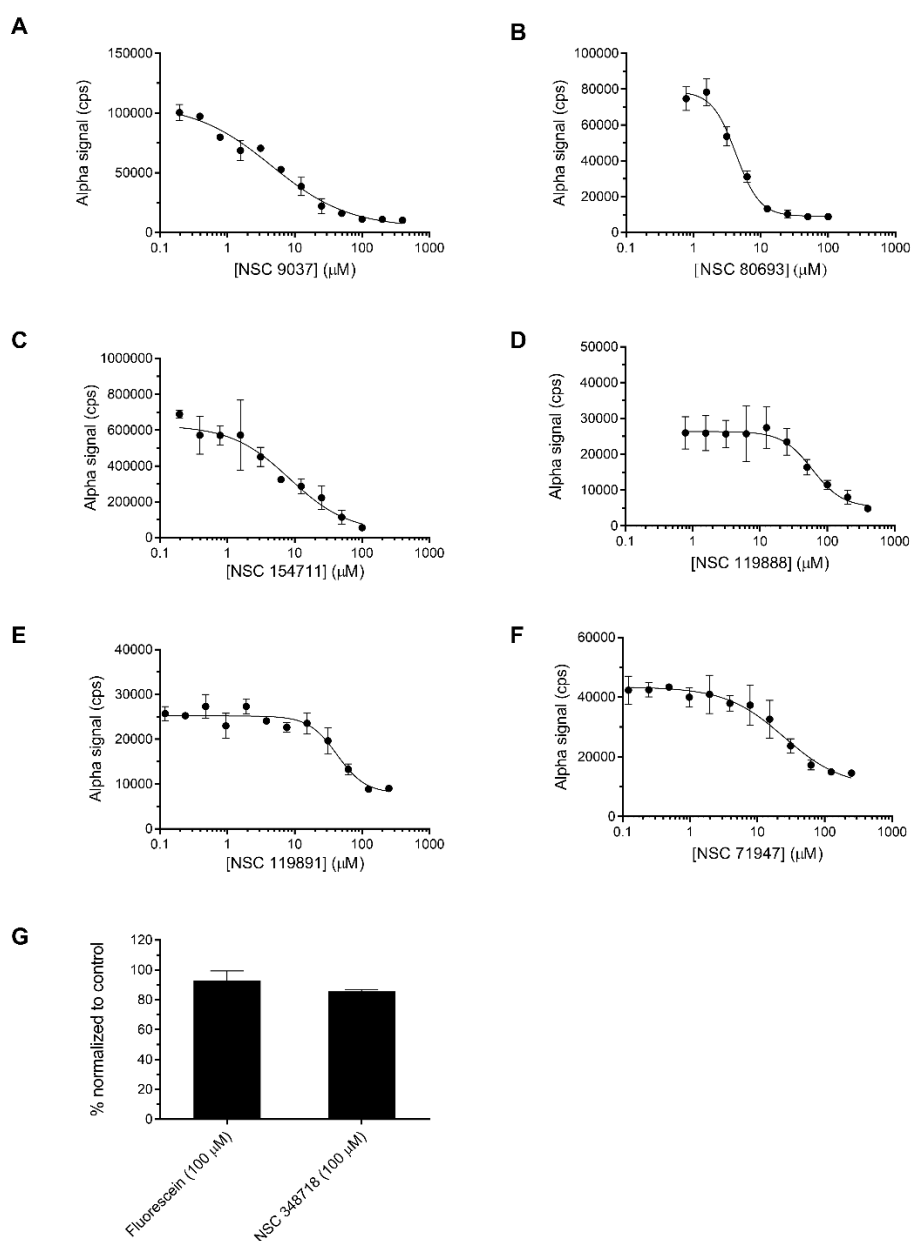


Figure 9 Dose-response for PCNA ubiquitination in the presence of compounds by alpha assay

(A) Dose response of NSC 9037 for PCNA ubiquitination. (B) Dose-response of NSC 80693 for PCNA ubiquitination. (C) Dose-response of NSC 154711 for PCNA ubiquitination. (D) Dose-response of NSC 119888 for PCNA ubiquitination. (E) Dose-response of NSC 119891 for PCNA ubiquitination. (F) Dose-response of NSC 71947 for PCNA ubiquitination. Curves in (A)-(F) were fitted by nonlinear regression and graphed semi-logarithmically. (G) Bar graph representation of the inactive compounds, fluorescein, and NSC 348718. Data represent mean with SD for triplicate samples in each case.

4.6. Dose-response analysis for Rad6~ubiquitin thioester formation

Dose-response experiments were carried out on Rad6~ubiquitin thioester formation, which is the second step in the PCNA ubiquitination cascade. All eight compounds were tested to determine the target protein in the PCNA ubiquitination cascade using the previously mentioned conditions for the ALPHA assay (Figure 10). We also confirmed our ALPHA assay results with a gel-based approach using silver staining for visualisation (Supplementary Figures 1, 2, and 3).

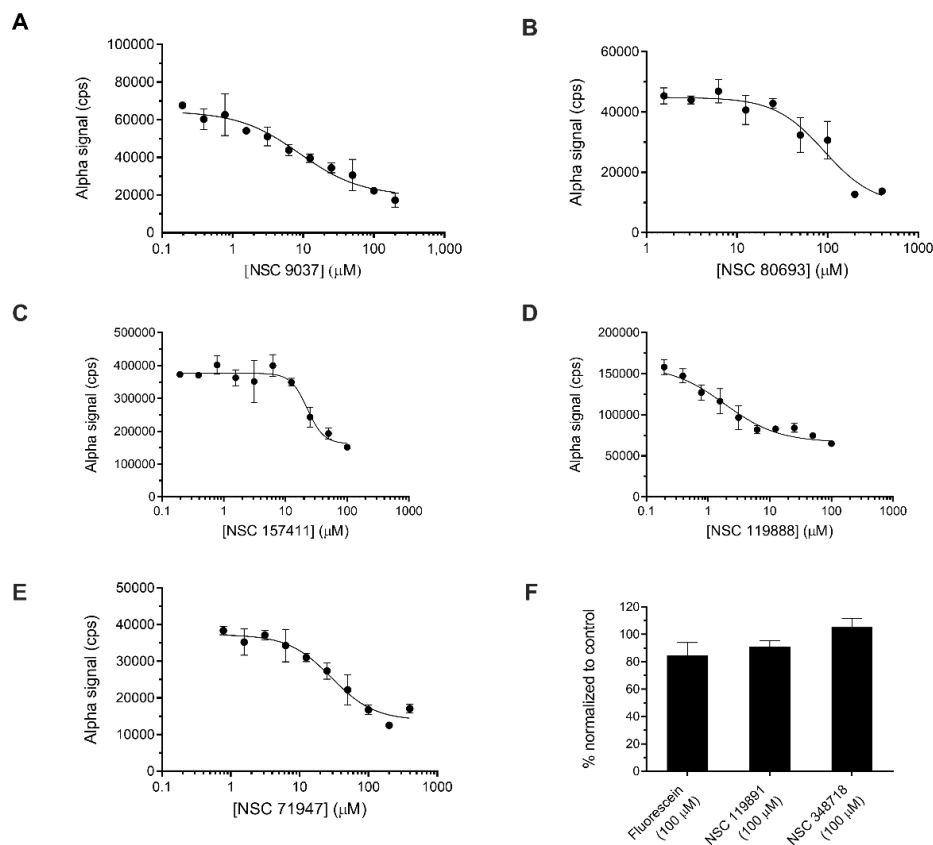


Figure 10 Dose-response for Rad6~ubiquitin thioester formation in the presence of compounds by Alpha assay

(A-F) shows the dose-response curve of NSC 9037, NSC 80693, NSC 157411, NSC 119888, and NSC 71947. Data represent mean with SD for triplicate samples in each case. Semilogarithmic plots are graphed (A-E). (F) Bar graph representation of inactive compounds Fluorescein, NSC 119891, and NSC 348718.

We found that a number of the xanthene-3-ones tested – NSC 9037, NSC 80693, NSC 157411, and NSC 119888, as well as the acridine NSC 71947 – inhibit the formation of the Rad6~ubiquitin thioester conjugate, while fluorescein, NSC 119891, and NSC 348718 do not inhibit this activity (Figure 10 A-F and Table 1).

To further confirm the Rad6 inhibition, we tested the compounds in a Rad18 autoubiquitination assay, which depends on Rad6 activity, and found that the NSC 9037, NSC 80693, and NSC 157411 compounds inhibit Rad18 autoubiquitination (Figure 11 A-D and Table 1).

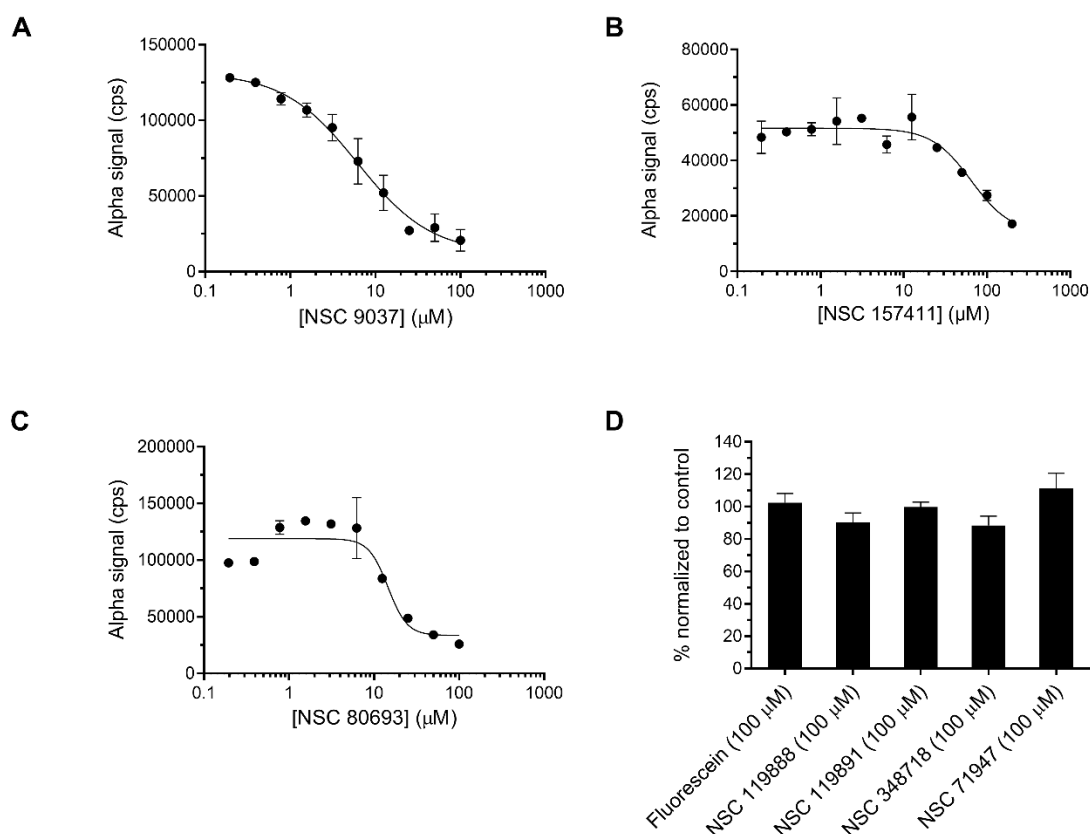


Figure 11 Dose-response for autoubiquitination of Rad18 in the presence of compounds by Alpha assay.

(A)-(C) shows the dose-response curve of NSC 9037, NSC 80693, and NSC 157411. **(A)-(C)** were fitted by nonlinear regression and graphed semi-logarithmically. Data represent mean with SD for triplicate samples in each case. **(D)** Bar graph representation of inactive compounds, fluorescein, NSC 119888, NSC 119891, NSC 71947, and NSC 348718.

However, after testing these compounds in the Uba1~ubiquitin thioester formation assay, we found that some of these compounds (NSC 157411 and NSC 119888) appeared less specific to Rad6 inhibition because of their inhibition of Uba1~ubiquitin thioester formation (Figure 12 and Table 1). Which shows that NSC 9037, NSC 80693, NSC 119891, Fluorescein, NSC 348718 and NSC 71947 are specific to Rad6.

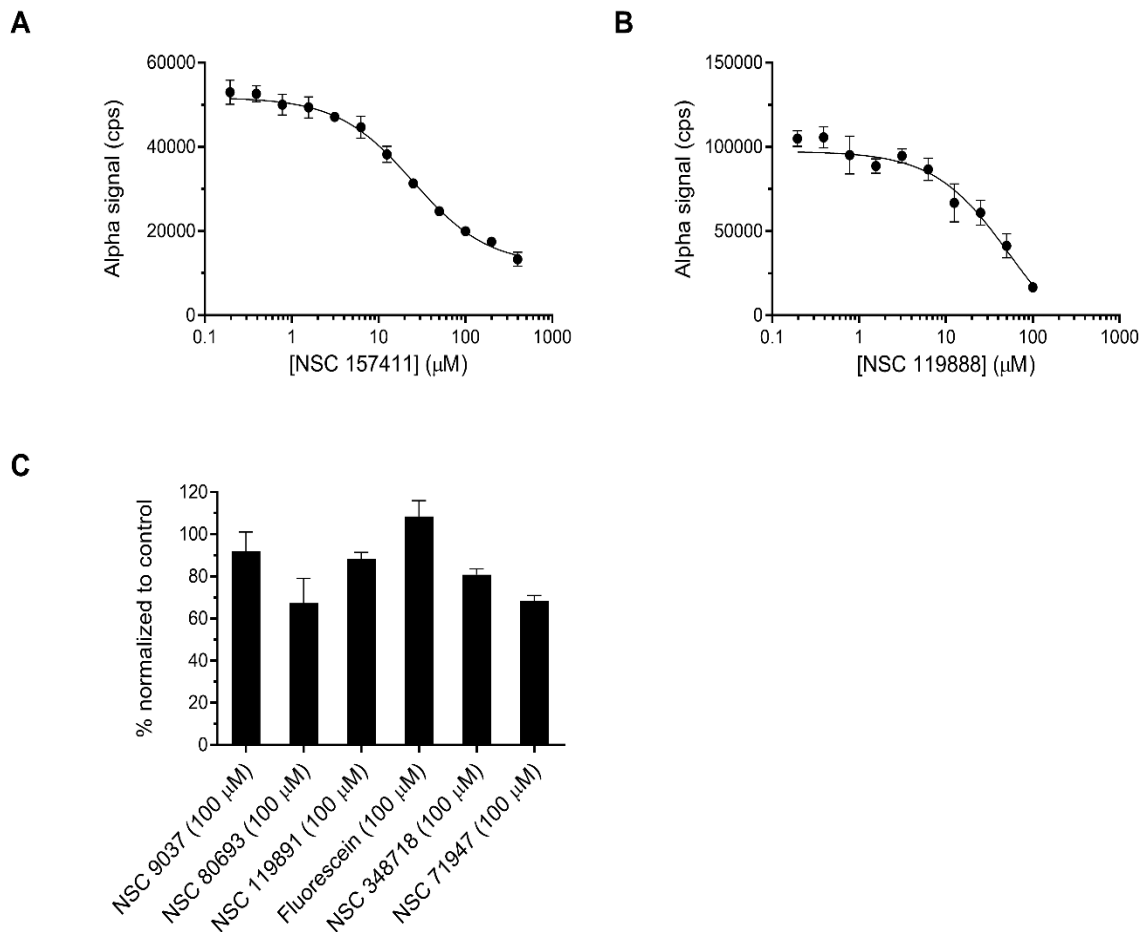


Figure 12 Dose-response for Uba1~ubiquitin thioester formation in the presence of compounds by Alpha assay

(A-B) shows the dose-response curves of NSC 157411 and NSC 119888. **(C)** Bar graph representation of inactive compounds, NSC 9037, NSC 80693, NSC 119891, Fluorescein, NSC 348718, and NSC 71947. Data represent mean with SD for triplicate samples in each case. Semilogarithmic plots are graphed **(A-B)**.

4.7. Dose–response for the Rad6–Rad18 interaction in the presence of compounds.

Rad6 is found in a complex form with Rad18, and the complex is responsible for catalysing the transfer of ubiquitin to the K164 residue of (PCNA). Rad6 and Rad18 interact via the RING domain situated near Rad18's N-terminus (Huang et al., 2011) and the Rad6-binding domain (Rad6BD) found near Rad18's C-terminus (Bailly et al., 1997; Hibbert et al., 2011; Notenboom et al., 2007).

Rad6's interaction with Rad18 inhibits its ability to form polyubiquitin chains, allowing only single ubiquitin moieties to be attached to PCNA (Bailly et al., 1997). Compounds that bind to Rad6 can inhibit its binding to Rad18 in addition to its ubiquitin-conjugating activity.

To examine this possibility, we tested the compounds in a Rad6–Rad18 interaction assay and discovered that a subset of the xanthene-3-ones hindered the association between Rad6 and Rad18 (Figure 13A-C and Table 1). We found that three of the xanthene-3-ones tested – NSC 9037, NSC 80693, and NSC 157411 – disrupt the Rad6–Rad18 interaction, while the rest of the xanthene-3-ones (NSC 119888, NSC 119891, and fluorescein), the non-ketone xanthene NSC 348718, and the acridine NSC 71947 do not appreciably inhibit the formation of the Rad6–Rad18 complex (Figure 13D). Fluorescein had no activity in any of the assays. These results were confirmed in a pulldown assay using Flag-Rad18 and GST-Rad6 (Supplementary Figure 4).

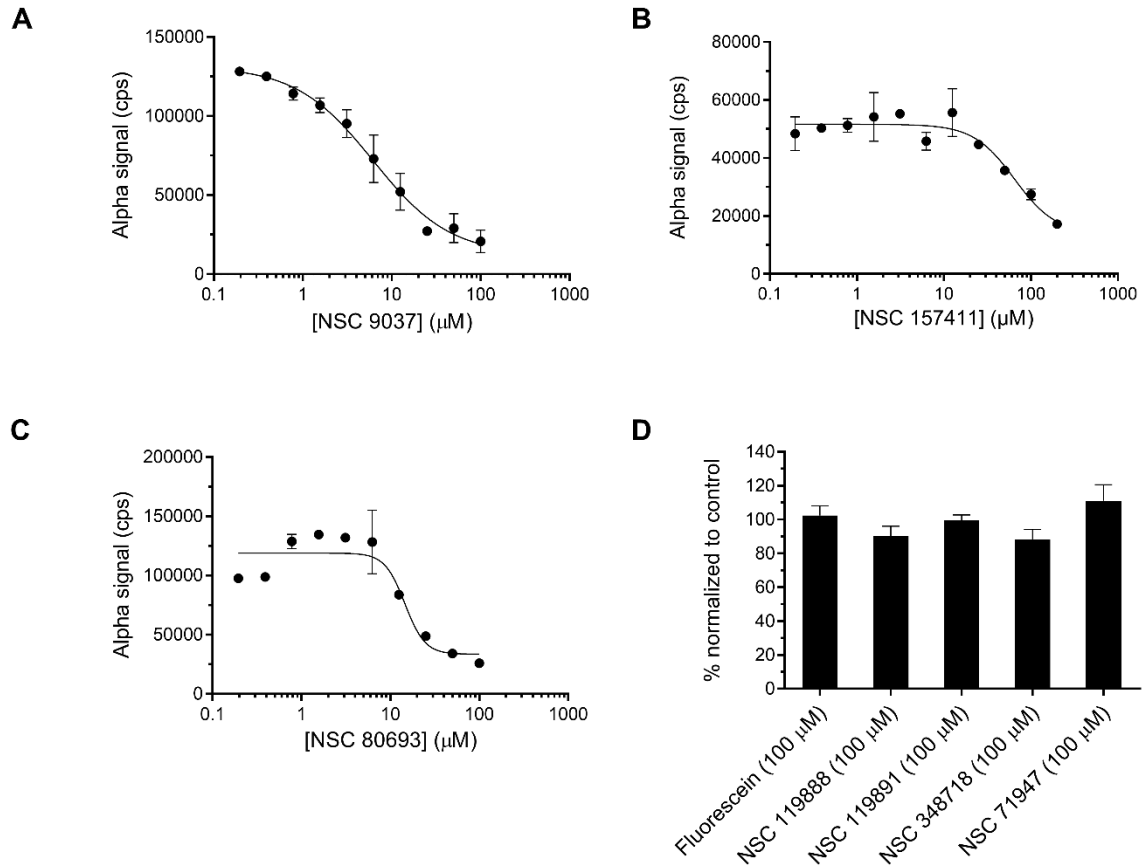


Figure 13 Dose–response for the Rad6–Rad18 interaction in the presence of compounds.

(A–C) shows the dose-response curve of NSC 9037, NSC 157411, and NSC 80693 inhibition of Rad6-Rad18 interaction. Data represent mean with SD for triplicate samples in each case. **(D)** Bar graph representation of inactive compounds fluorescein, NSC 119888, NSC 119891, NSC 348718, and NSC 71947. Semilogarithmic plots are graphed **(A–C)**.

As for determining the selectivity of our compounds, we tested our most potent compound, NSC 9037, on a gel-based Rad6 interaction assay with another E3, Ubr1, a ubiquitin ligase in N-end rule pathway, which regulates the *in vivo* half-life of a protein to the identity of its N-terminal residue (Hwang et al., 2010) and found no significant inhibition (Supplementary Figure 3B) and no or minimum effect of the other examined compounds as revealed by our Alpha assay (Figure 14).

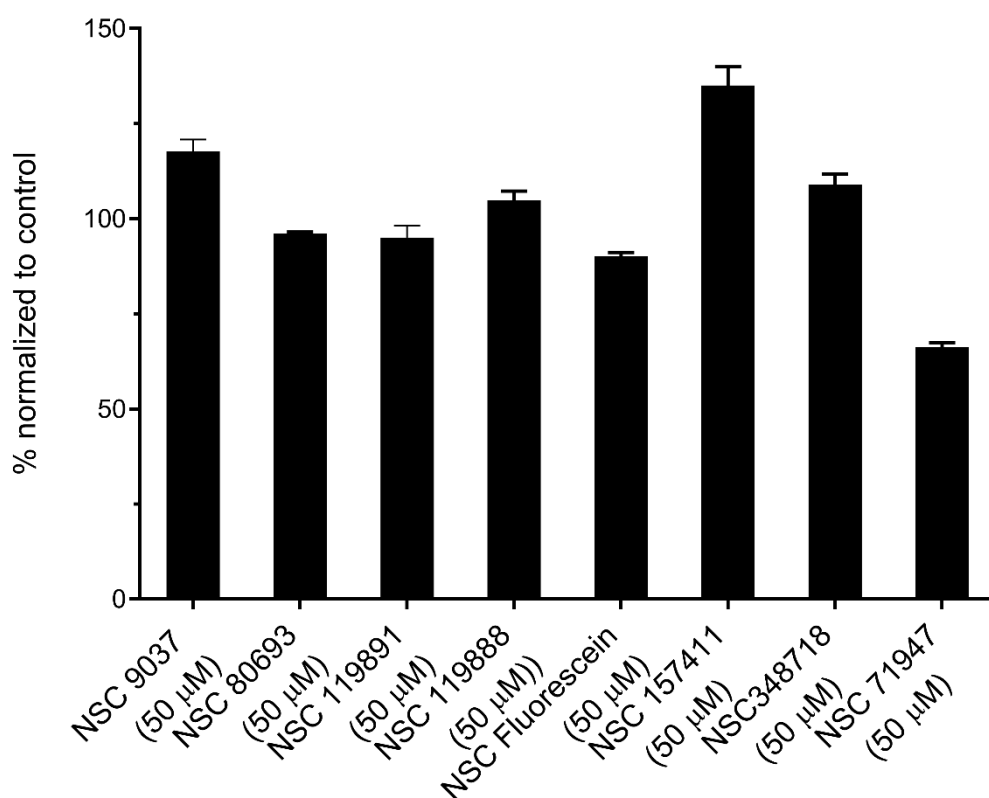


Figure 14 Rad6-Ubr1 ALPHA assay

Rad6-Ubr1 interaction assay in the presence of compounds at a final concentration of 50 μM. All the compounds showed weak to no inhibition of Rad6-Ubr1 interaction. Bar graph representation of compounds, NSC 9037, NSC 80693, NSC 119891, NSC 119888 Fluorescein, NSC 157411, NSC 348718 and NSC 71947. Data represent mean with SD for triplicate samples in each case.

Using a gel-based experiment, we also examined the impact of the drugs on the formation of ubiquitin conjugates with a heterodimeric ubiquitin-conjugating E2 enzyme, the Mms2-Ubc13 E2 (Supplementary Figure 3A), which catalyses K63 specific polyubiquitination of PCNA, and found that these compounds do not tend to inhibit all E2 enzymes.

4.8. Confirming target-protein binding using microscale thermophoresis (MST)

To further explore the target binding protein of NSC 9037, the most specific and highly potent inhibitor of PCNA ubiquitination of the examined compounds, we tested it on microscale thermophoresis (mentioned in the methods section). MicroScale Thermophoresis, also known as MST, is an effective method for quantifying the interactions between biomolecules. It is based on the principle of thermophoresis, which is a directed movement of molecules in a temperature gradient. This movement heavily depends on a range of molecular parameters such as size, charge, hydration shell, or conformation. Therefore, this method is extremely sensitive to nearly any change in molecular characteristics, and it enables accurate quantification of molecular events regardless of the size or nature of the material that is being analysed.

The dissociation constant (K_d) of NSC 9037 binding to Rad6 was determined to be $3.79 \pm 2.94 \mu\text{M}$ (mean \pm standard deviation) through our calculations (Figure 15). However, NSC 9037 demonstrated minimal binding affinity towards Rad18 at the low concentrations utilized in the Rad6-binding analysis. The measurement of the K_d value for NSC 9037-Rad18 binding was challenging due to the fluorescence of the compound at higher concentrations, which interfered with the green wavelength excitation utilized in our microscale thermophoresis device. MST experiment showed strong binding of NSC 9037 to GFP-Rad6.

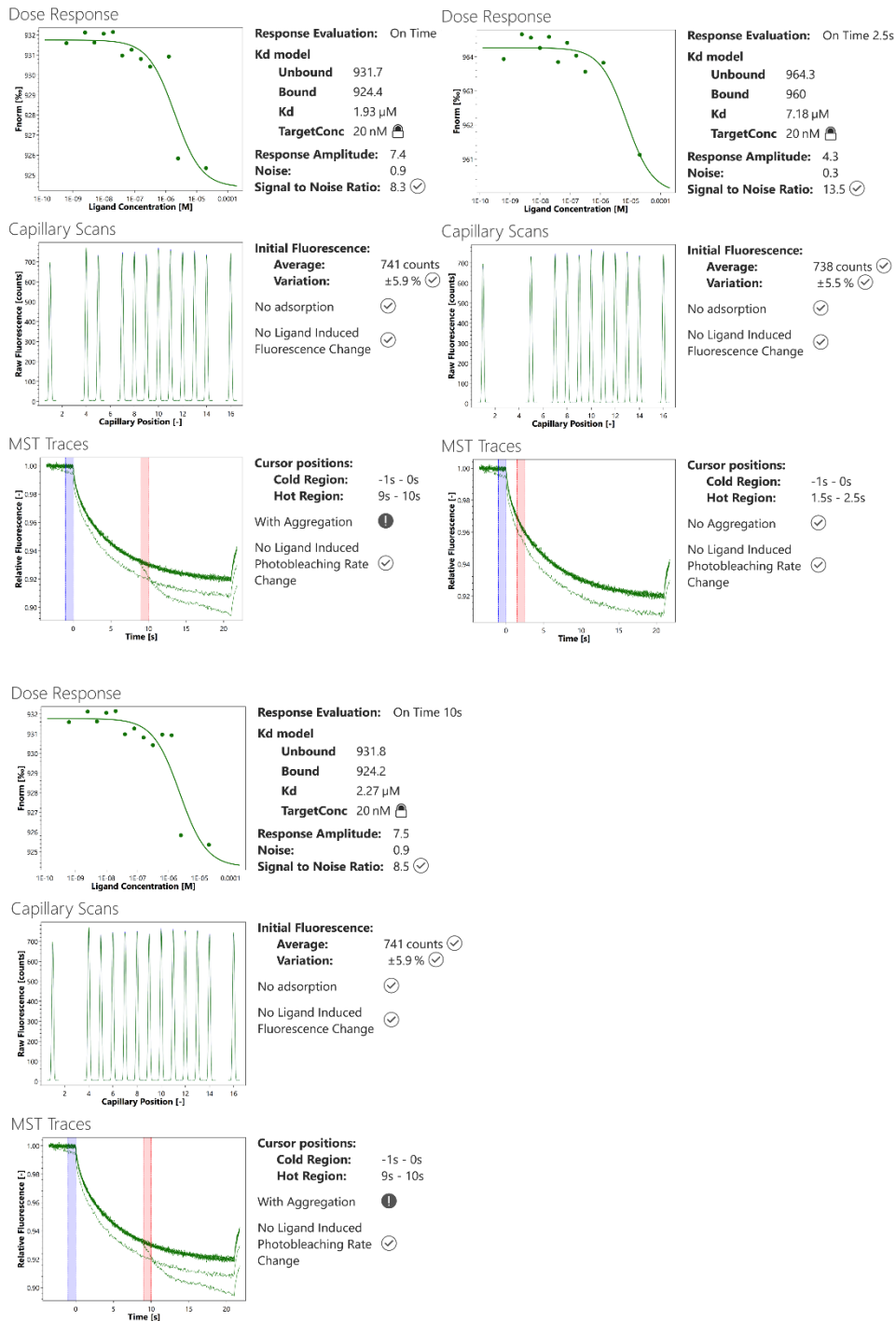


Figure 15 Microscale thermophoresis experiment.

NSC 9037 was tested using MST to determine the Kd. Triplicate experiments were performed using GFP-Rad6. These raw data were used to calculate the Kd for the interaction of NSC 9037 with Rad6, determined to be $3.79 \pm 2.94 \mu\text{M}$ (mean \pm SD) from three independent experiments.

4.9. Dose-response analysis of cell survival

To check the effects of compounds on cell survival, we tested all the compounds in HeLa cells in 96-well cell culture plates at a density of 1×10^4 cells in 50 μ l per well in DMEM containing 0.5% FBS at 37°C and 5% CO₂. The cells were treated for 24 h with compounds, and after that, resazurin (Alamar Blue) was added. Alamar Blue is a redox indicator that is used to measure the metabolic activity of cells. The metabolic activity of cells is directly proportional to the amount of Alamar Blue that is reduced, which can be quantified using spectrophotometry. The colour change was measured 4 h later on a fluorescence plate reader with excitation of 570 nm and emission of 585 nm.

The compounds exhibited variable effects on cell survival (Figure 16 and Table 1). Fluorescein did not affect cell viability, while the other compounds ranged from mild effects that plateaued at a partially inhibited condition to complete cytotoxicity at relatively low concentrations.

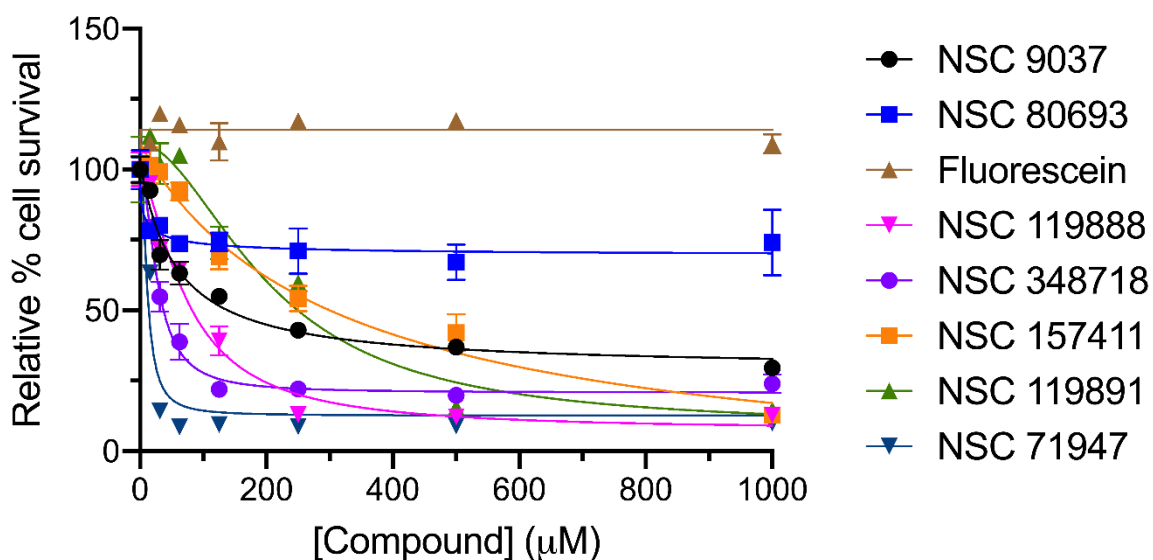


Figure 16 Effect of compounds on the viability of HeLa cells

Dose-response analysis to determine the effects of compounds on HeLa cells' survival. Data represent mean with SD for triplicate samples in each case. Semilogarithmic plots are graphed.

4.10. Identification of possible compound-binding sites

To identify the possible NSC 9037 binding site on Rad6B, we first docked it to the nuclear magnetic resonance (NMR) solution structure of human Rad6B (PDB ID: 2Y4W, Huang, et al., 2011). Two putative binding sites for NSC 9037 have been found on the surface of Rad6. In Figure 17A, these sites and two representative binding orientations are depicted. The refinement of these binding positions was achieved by undertaking flexible blind dockings. Flexible docking is a computational approach used to predict how small molecule ligands, such as drug candidates, bind to a protein receptor. Since both the protein receptor and the ligand can adopt multiple conformations and orientations, flexible docking typically involves searching through a large number of possible combinations to identify the most favorable binding mode.

In addition, all eight xanthene derivatives have been included in the flexible blind dockings. The results for the entire set of compounds confirmed the location of the above-mentioned probable binding sites (SN-SN+7; Figure 17B and Table 2).

Residues D12 and S60 were identified to form the most polar interactions at site 1, while the most frequent hydrophobic contacts were formed with residues F59, P64, P68, and W96. Y130 and Y137 were responsible for the polar contacts at site 2, while I105 and V141 were mostly responsible for the hydrophobic interactions. The observed presumably false positive prediction for a few of the compounds reflects the limitations of the docking method to differentiate between compounds with similar structures and polarity. Whereas geometric features are well accounted for, differences between polar functional groups in forming intermolecular interactions are roughly approximated. The results suggest two potential binding sites for the compounds, and either one or both of these sites appear to be occupied by all of the compounds. The proposed binding sites for the compounds are situated distantly from

the catalytic cysteine residue, namely C88 in human Rad6B, which plays a crucial role in thioester formation with ubiquitin. This finding implies that, if the predicted outcome holds true, inhibition of Rad6~ubiquitin thioester formation occurs through an allosteric mechanism involving extensive conformational alterations. Regarding the interaction between Rad6 and Rad18, the two presumed binding sites of the compounds are located on opposite ends of Rad6's Rad6BD-binding site. Additionally, Rad6BD coincides with Rad6's noncovalent binding site for ubiquitin. It is conceivable that binding of the compounds could cause alterations in the nearby molecular structure, leading to changes in the distribution of partial atomic charges that would decrease the affinity of Rad6 for Rad6BD.

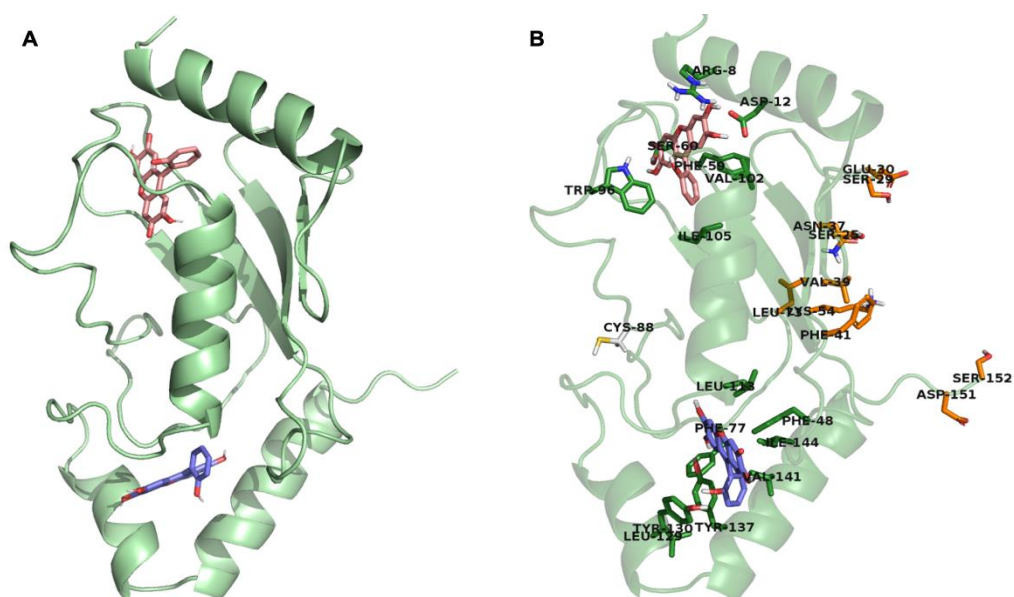


Figure 17 Computational docking of NSC 9037 to Rad6B

(A) Potential binding sites and poses (shown in pink and purple) (different possible orientations and conformations of a ligand molecule relative to a protein receptor that could lead to a stable binding interaction). of NSC 9037 on Rad6 identified by initial blind dockings of flexible compounds to rigid protein surfaces. **(B)** Refined binding poses of NSC 9037 (shown in pink and purple) on Rad6 resulting from flexible blind dockings. Amino acid residues in contact with NSC 9037, which were both kept flexible during this second round of dockings, are shown in green. Those in close proximity to the putative compound-binding sites and involved in Rad18's Rad6BD–Rad6 interactions are shown in orange. The catalytic cysteine residue (C88) on Rad6 is shown in white. These analyses were extended to all the compounds, and predicted K_i values and specific contacts with amino acid residues on Rad6 are listed in **Table 2**.

Compound	Grid (site)	K_i (nM)	Polar contacts	Hydrophobic Contacts
NSC 9037	1	0.1	R ⁸ , D ¹² , S ⁶⁰	L ⁹ , F ⁵⁷ , F ⁵⁹ , P ⁶⁴ , P ⁶⁸ , W ⁹⁶ , V ¹⁰² , I ¹⁰⁵
	2	90.2	H ⁷⁸ , Y ¹³⁰ , Y ¹³⁷	P ⁴⁷ , F ⁴⁸ , P ⁷⁹ , L ¹¹³ , P ¹¹⁶ , V ¹⁴¹
NSC 80693	1	< 0.1	R ⁸ , D ¹² , S ⁶⁰	L ⁹ , F ⁵⁹ , P ⁶⁴ , P ⁶⁸ , I ¹⁰⁵
	2	24.5	Q ¹²⁵ , Y ¹³⁰	F ⁷⁷ , V ⁸¹ , I ¹⁰⁵ , L ¹²⁹ , Y ¹³⁷ , V ¹⁴¹
NSC 119891	1	7.8	–	F ⁵⁹ , P ⁶⁴ , P ⁶⁸ , W ⁹⁶ , I ¹⁰⁵
	2	11.4	H ⁷⁸ , Y ¹³⁰ , Y ¹³⁷	P ⁴⁷ , F ⁴⁸ , P ⁷⁹ , V ¹⁴¹
NSC 119888	1	0.7	S ⁶⁰	F ⁵⁹ , P ⁶⁸ , W ⁹⁶ , I ¹⁰⁵
	2	0.9	Y ¹³⁰ , Y ¹³⁷	P ⁴⁷ , F ⁷⁷ , P ⁷⁹ , L ¹¹³ , P ¹¹⁶ , L ¹²⁹ , V ¹⁴¹
Fluorescein	1	2.0	D ¹² , S ⁶⁰ , D ¹⁰¹	F ⁵⁹ , P ⁶⁸ , W ⁹⁶ , V ¹⁰² , I ¹⁰⁵
	2	26.2	Y ¹³⁰ , R ¹⁴⁰	F ⁷⁷ , L ¹²⁹ , V ¹⁴¹
NSC 157411	1	1.1	R ⁸ , D ¹² , S ⁶⁰	F ⁵⁹ , P ⁶⁴ , P ⁶⁸ , W ⁹⁶ , I ¹⁰⁵
	2	0.9	Y ¹³⁰ , Y ¹³⁷	P ⁴⁷ , F ⁴⁸ , F ⁷⁷ , P ⁷⁹ , P ¹¹⁶ , V ¹⁴¹
NSC 348718	1	1.7	D ¹² , S ⁶⁰ , D ¹⁰¹	R ⁸ , F ⁵⁹ , P ⁶⁴ , P ⁶⁸ , W ⁹⁶ , I ¹⁰⁵
	2	19.3	–	P ⁴⁷ , F ⁴⁸ , P ⁷⁹ , P ¹¹⁶ , Y ¹³⁰ , Y ¹³⁷ , V ¹⁴¹
NSC 71947	1	66.4	S ⁶⁰	R ⁸ , F ⁵⁹ , P ⁶⁴ , P ⁶⁸ , V ¹⁰² , I ¹⁰⁵
	2	92.2	Y ¹³⁰	P ⁷⁹ , L ¹¹³ , P ¹¹⁶ , Y ¹³⁷ , V ¹⁴¹

Table 2 *In silico* binding affinities and amino acid side chains of human Rad6B in contact with the tested ligands, obtained from refined docking of flexible compounds to flexible protein surfaces.

The table includes binding sites with their respective K_i (nM) values and polar and hydrophobic contacts of all the compounds.

5. Discussion

We have developed, optimised, and implemented multiple robust and quantitative, high-throughput *in vitro* assays for the PCNA ubiquitination cascade. PCNA ubiquitination at a particular lysine residue (K164) activates multiple DNA damage tolerance mechanisms. Our assays are based on the amplified luminescent proximity homogeneous assay (ALPHA). We took our previously optimised western blot conditions for PCNA ubiquitination (50 nM Uba1, 50 nM RFC, 50 nM FLAG-PCNA, 250 nM biotin-ubiquitin, 250 nM Rad6-Rad18, 2 mM ATP and 2.5 nM DNA) as a reference and then developed and optimised ALPHA assay for each step involved in PCNA ubiquitination (Uba1~ubiquitin thioester formation, Rad6~ubiquitin thioester formation, Rad18 auto-ubiquitination, and Rad6-Rad18 interaction). We compared and validated the optimised condition (10 nM Uba1, 10 nM RFC, 50 nM FLAG-PCNA, 100 nM biotin-ubiquitin, 100 nM Rad6-Rad18, 2 mM ATP, and 2 nM DNA) of ALPHA assay for PCNA ubiquitination by the western-blot technique (Figure 6B) and found comparable results. The optimisation of protein and bead concentrations, as well as other parameters, is critical in the implementation of an Alpha-based screening effort in order to use economic amounts of proteins and beads while maintaining high signal strength and dynamic range.

The ALPHA system is based on the luminescent oxygen channelling immunoassay, a homogeneous bead-based immunoassay method. Upon irradiation by high energy at 680 nm wavelength, the phthalocyanine in the Alpha donor beads, which is a photosensitiser, excites and converts the ambient ground-state oxygen to an excited singlet state. This singlet oxygen has a half-life of 4 μ s, and it can travel up to 200 nm distance. Within this range, singlet oxygen can react with a thioxene derivative in an Alpha acceptor bead, creating a chemiluminescent emission that excites fluors also

present in the acceptor beads resulting in fluorescent emissions at 520–620 nm in the case of Alphascreen and 615 nm in AlphaLisa, which is then detected by a photomultiplier tube. When the distance between the donor and acceptor beads is more than 200 nm, the excited singlet oxygen falls to the ground state, and no signal is produced. Experiment to experiment, the specific signal intensity values of the range (e.g., between the minimum and maximum signal values or between negative and positive control values) can vary, even under tightly controlled identical conditions. Therefore, substantial normalisation is required prior to integrating data from multiple independent experiments (Fenteany et al., 2020). The alpha assay is sensitive to the high-dose hook effect, wherein excessive analyte concentrations attenuate signals in bimolecular detection assays, also known as the “hooking” or “prozone” effect. Its name comes from the hook-like profile formed by the concentration versus signal plot for the analyte.

We screened multiple different small molecule libraries, including the Diversity Set VI from the US National Cancer Institute’s Developmental Therapeutics Program (DTP), and have identified and found a series of xanthenes and a related acridine derivative (NSC 71947), a compound family that we describe here as inhibitors of PCNA ubiquitination, Rad6~ubiquitin thioester formation, and Rad6-Rad18 interaction. This last activity is novel for a small molecule. The compounds which possess inhibitory activity are a subset of xanthene-3-ones, while other xanthene-3-ones and related compounds do not have inhibitory activity. It has been previously reported that xanthene derivatives have been shown to have a range of medicinal properties, such as potential neuroprotective, antitumor, and antibacterial activities, among others (Ghahsare et al., 2020; Maia et al., 2021). A subset of these compounds (NSC 9037, NSC 157411, and NSC 80693) inhibits Rad6~ubiquitin thioester formation and

disrupts Rad6–Rad18 interaction, a key step required for the monoubiquitination of PCNA at the lysine K164 site, which initiates the pathways of DNA damage bypass and tolerance. It is anticipated that inhibiting the more downstream steps of the PCNA ubiquitination cascade will result in a more selective decrease of DNA damage tolerance than inhibiting other ubiquitin- or UBL-based pathways. Ubiquitin and related ubiquitin-like proteins (UBLs) function as tags and docking sites for interactions with other proteins and the assembly of massive protein complexes that govern a vast array of physiological processes. Utilising small molecule inhibitors or activators/enhancers to modulate various phases of the ubiquitination and UBL post-translational modification pathways has significant research and therapeutic potential.

The inhibitory compounds that we have described in our study share a structural similarity with other xanthene dyes, such as rhodamine and eosin, as well as fluorescein, which we found to be ineffective in our assays. These compounds display inhibitory activity against the formation of Rad6~ubiquitin thioester, and some of them also disrupt the interaction between Rad6 and Rad18. Rad18 is a RING class E3 protein ligase that has a limited range of target substrates, primarily PCNA on its K164 residue. The most “druggable” as both direct and indirect target in PCNA ubiquitination is probably Ub1, the ubiquitin-activating enzyme, which is responsible for the first step in virtually all ubiquitination pathways based on our (Fenteany et al., 2020, 2019) and others’ (An and Statsyuk, 2015, 2013; Hann et al., 2019; Hong and Luesch, 2012; Hyer et al., 2018; Lu et al., 2010; Sekizawa et al., 2002; Tsukamoto et al., 2005; Ungermannova et al., 2013, 2012a, 2012a; Xu et al., 2010; Yamanokuchi et al., 2012; Yang et al., 2007) empirical experience, as well as structural and docking studies, with at least four putative general compound-binding hot spot pockets, as computationally predicted (Lv et al., 2018). There is just one known family of inhibitors that can inhibit

the formation of the Rad6-ubiquitin thioester conjugate (Haynes et al., 2020, 2016, 2015; Saadat et al., 2018; Sanders et al., 2017, 2013), despite the fact that there are quite a few distinct Uba1 inhibitors (An and Statsyuk, 2015, 2013; Fenteany et al., 2019; Hann et al., 2019; Hong and Luesch, 2012; Hyer et al., 2018; Sekizawa et al., 2002; Tsukamoto et al., 2005; Ungermannova et al., 2013, 2012a, 2012b; Xu et al., 2010; Yamanokuchi et al., 2012; Yang et al., 2007). No compound has yet been reported that interferes with the association of Rad6 with Rad18.

Based on the preliminary structure-activity relationships, specific groups and their positioning are crucial for activity. Initial investigations into the structure-activity relationships have revealed that positioning particular groups within the structure is crucial for the activity. The compounds exhibit different selectivities in different assays (Figures 9-14 and Table 1), with only a subset of the xanthene-3-ones, but not the other xanthenes or the acridine derivative, inhibiting the Rad6–Rad18 interaction (Figure 13). Fluorescein, the ortho-substituted constitutional isomer of NSC 119891 and NSC 119888, had no activity in any of these assays. The meta- and para-substituted isomers (NSC 119888 and NSC 119891, respectively) were biologically active in a number of the assays. The results indicate that the positioning of the carboxylic acid group in isomeric xanthene-3-ones plays a crucial role in determining their activity. Fluorescein, with its carboxylic acid group in the ortho position of the phenyl ring, can undergo cyclization to a phthalein product. Furthermore, NSC 157411, which contains a cyclohexene group in place of the phenyl ring, also demonstrates biological activity. The selective activities of the bioactive compounds against different proteins suggest that these molecules are not simply pan-assay interference compounds, whose effects could be attributed to colloidal aggregation.

However, some of these compounds were observed to aggregate at higher concentrations over time.

Microscale thermophoresis reveals that NSC 9037 binds to Rad6 with a K_d of 3.79 μM (Figure 15). NSC 9037 also possesses the highest affinity for Rad6 out of all of the compounds that were tested using blind docking. The computational results suggest two potential binding sites for the compounds, and either one or both of these sites appear to be occupied by all of the compounds (Table 2). The fact that these two putative compound-binding sites are not located close to the catalytic cysteine residue that is involved in thioester formation with ubiquitin (C88 in human Rad6B) suggests that, if the predictions are accurate, the inhibition of Rad6-ubiquitin thioester formation is exerted through an allosteric mechanism that involves significant conformational changes. Comparing these probable compound-binding sites to the C-terminal location of the Rad6-binding domain (Rad6BD) on Rad18, which is one of the major interfaces of contact between Rad6 and Rad18 (Bailly et al., 1997; Hibbert et al., 2011; Notenboom et al., 2007), as shown in an X-ray co-crystal structure [(PDB ID: 2YBF) (Hibbert et al., 2011)], we observed that the two putative binding sites for the compounds lie on either side of the Rad6BD-binding site on Rad6. The Rad6BD also overlaps with the noncovalent ubiquitin-binding of Rad6 (Hibbert et al., 2011). It is not difficult to imagine that the binding of compounds may result in local conformational changes and, as a consequence, changes in the local distribution of partial atomic charges. These alterations would have the effect of reducing the affinity of Rad6 for the Rad6BD. Interactions between Rad6-Rad18 are also affected by the RING domain that is found close to the N-terminus of Rad18 (Huang et al., 2011; Masuda et al., 2012; Notenboom et al., 2007). This protein domain–protein domain interaction site is also on the same face of the protein as the potential binding sites for the drugs, which

indicates that this interaction may also be influenced by the compounds when they bind to the protein.

The core structure of the xanthene-3-ones may be a key determinant of their activity against the interaction between Rad6 and Rad18, as all of the compounds that have been shown to disrupt this interaction are xanthene-3-ones. However, not all xanthene-3-ones possess this ability. Similarly, all of the compounds that have been shown to inhibit the formation of a thioester between Rad6 and ubiquitin are xanthene-3-ones, but only a subset of these also inhibit the Rad6-Rad18 interaction and the Rad6-ubiquitin thioester formation.

These findings suggest that the xanthene-3-one structure is necessary but not sufficient for activity against the Rad6-Rad18 interaction and the Rad6-ubiquitin thioester formation. Additional factors, such as the specific functional groups attached to the xanthene-3-one core, may play a role in determining the compounds' activity. It is also possible that the compounds induce significant conformational changes in Rad6, as the active site cysteine (C88 in human Rad6B) and the regions of interaction with Rad18 are located on opposite faces of the protein. Further studies will be needed to fully understand the molecular basis of these compounds' activity.

6. Summary

Cells are subjected to many forms of genotoxic stress, which can cause mutations and contribute to cancer. Cancer remains a serious health concern after many years of research, and standard treatments such as chemotherapy, radiation, and surgery have limitations, including difficulty in discriminating between cancerous and healthy cells, which results in significant toxicity and side effects. In order to repair DNA damage, cells use various methods such as base-excision repair (BER), nucleotide excision repair (NER), homologous recombination (HR), and non-homologous end joining (NHEJ), but sometimes the damage is left unrepaired during the DNA replication and it stalls the progressing replication fork in the S phase of the cell cycle. At the stalled replication fork, PCNA undergoes monoubiquitination at lysine residue K164. The monoubiquitination of PCNA is achieved through the combined action of two enzymes, Rad6 and Rad18. Rad6 acts as an E2 ubiquitin-conjugating enzyme and catalyses the attachment of ubiquitin to PCNA, while Rad18 acts as an E3 ubiquitin ligase and provides specific recognition of PCNA as a substrate. This process begins with the ATP-dependent binding of PCNA to DNA by the RFC protein. Monoubiquitination serves as a trigger mechanism to bring in specialized DNA polymerases, called translesion synthesis (TLS) polymerases. These polymerases are involved in replication that is prone to errors, leading to mutagenesis and potential carcinogenic outcomes. This form of DNA repair, involving the use of TLS polymerases, is referred to as translesion DNA synthesis.

To address these constraints, there has been a surge in interest in the development of small compounds for cancer treatment. These compounds are preferred because of their capacity to quickly cross the plasma membrane and interact with cell-surface receptors and intracellular signaling molecules. They typically have a molecular weight

of less than 900 Da. We have concentrated on small compounds that target ubiquitin's post-translational modification of the proliferating cell nuclear antigen (PCNA).

In the first phase of our project, we focused on developing and optimising a range of robust, reliable high-throughput assays based on the luminescent proximity homogeneous assay (ALPHA) technology. These assays allowed us to investigate each sequential step in the PCNA ubiquitination cascade in detail. We also created specific assays, such as those for Uba1~Ubiquitin thioester, Rad6~Ubiquitin thioester, Rad18 autoubiquitination, and Rad6-Rad18 interaction, to further characterise our small molecule hits.

Utilizing these assays, we conducted screenings on different chemical libraries, including the US National Cancer Institute's Developmental Therapeutics Program Diversity Set VI, and discovered a particular group of compounds that exhibit potential as inhibitors of PCNA ubiquitination, Rad6~ubiquitin thioester formation, and the Rad6-Rad18 interaction. This novel activity for a small molecule has implications for further research on the molecular basis and therapeutic control of these processes.

We have identified a series of xanthenes that show potential as inhibitors of PCNA ubiquitination, and a subset of these also inhibit Rad6~ubiquitin thioester formation and disrupt the interaction between Rad6 and Rad18. Xanthenes, in addition to being dyes and pigments, have also been studied for their potential applications in various fields, including medicine, where they may have potential as anticancer or other therapeutic agents. These compounds may serve as a starting point for further medicinal chemistry efforts to improve their activity and investigate their potential therapeutic applications.

7. Összefoglaló

A sejteket számos genotoxikus stressz éri, mely mutációkat okozhat és daganatos megbetegedések kialakulásához vezethet. A tumoros megbetegedések sokévnnyi kutatást követően is komoly egészségügyi problémát jelentenek, és a hagyományos kezelések, mint például a kemoterápia, a sugárkezelés vagy a műtét, korlátozottan alkalmazhatók, többek között azért, mert nem képesek megkülönböztetni a rákos és az egészséges sejteket, ami jelentős toxicitást és mellékhatásokat eredményez.

A DNS-károsodások javítására a sejtekben különböző folyamatok fejlődtek ki, mint például a báziskivágó hibajavítás (BER), a nukleotidkivágó hibajavítás (NER), a homológ rekombináció (HR) és a nem homológ végek összekapcsolása (NHEJ), de előfordul, hogy a károsodás a DNS-replikáció során nem kerül kijavításra, és a replikációs villa a sejtciklus S fázisában elakad. Az elakadt replikációs villánál a PCNA monoubikvitinálódik a 164. pozíciójú lizinen. A PCNA monoubikvitinációjában két enzim, a Rad6 és a Rad18 együttese játszik szerepet. A Rad6 E2 ubikvitin-konjugáló enzimként működik, és az ubikvitin PCNA-hez való kötődését katalizálja, míg a Rad18 E3 ubikvitin ligáz, és a PCNA szubsztrátként történő felismerését biztosítja. Ez a folyamat a PCNA-nek az RFC fehérje általi, DNS-hez való kötődésével kezdődik, mely folyamat ATP-függő. A monoubikvitináció speciális DNS-polimerázok, úgynevezett transzléziós szintézis (TLS) polimerázok bevonását indítja el. Ezek a polimerázok a replikáció során hibák generálására hajlamosak, ami mutagenézishoz és potenciálisan tumorok kialakulásához vezethet. A DNS-javításnak ezt a TLS-polimerázok révén történő típusát transzléziós DNS-szintézisnek nevezik.

A terápiaik korlátainak leküzdésére tett erőfeszítések a rák kezelésére alkalmas kismolekulák kifejlesztése iránti érdeklődés megnövekedéséhez vezetett. Ezek a

molekulák azért előnyösek, mert képesek gyorsan átjutni a plazmamembránon és kölcsönhatásba lépni a sejtfelszíni receptorokkal és az intracelluláris jelzőmolekulákkal. Molekulatömegük jellemzően 900 Da-nál kisebb. Kísérleteink során olyan kis vegyületekre fókuszáltunk, amelyek a replikatív polimeráz processzivitási faktorának (PCNA) ubikvitin által történő, poszttranszlációs módosítását célozzák meg.

Projektünk első fázisában ALPHA (nagy jelerősítésű homogén távolság modulált lumineszcens assay) technológián alapuló, erőteljes, megbízható, nagy áteresztőképességű módszerek kifejlesztésére és optimalizálására összpontosítottunk. Ezek az assay-k lehetővé tették a PCNA ubikvitinációs kaszkád minden egymást követő lépésének részletes vizsgálatát. Specifikus assay-eket is létrehoztunk, például az Uba1~Ubiquitin tioészter, a Rad6~Ubiquitin tioészter, a Rad18 autoubikvitináció és a Rad6-Rad18 kölcsönhatás vizsgálatára, hogy tovább jellemezzük a kismolekulákat, melyeket kiszűrtünk.

A kifejlesztett assay-k segítségével különböző kémiai könyvtárakat vizsgáltunk, többek között az US National Cancer Institute's Developmental Therapeutics Program Diversity Set VI-ot, és azonosítottunk egy vegyületcsaládot, amely ígéretes eredményeket mutat a PCNA ubikvitináció, a Rad6~ubikvitin tioészter képződés és a Rad6-Rad18 kölcsönhatás gátlójaként. Ez eddig ismeretlen aktivitás egy kismolekula esetében, és ezek a vegyületek értékesnek bizonyulhatnak a fenti folyamatok molekuláris alapjainak és terápiás ellenőrzésének jövőbeli kutatásában.

Azonosítottunk egy sor olyan xantént, amelyek a PCNA ubikvitináció inhibitorai lehetnek, és ezek egy része gátolja a Rad6~ubikvitin tioészter képződést is, és megzavarja a Rad6 és a Rad18 közötti kölcsönhatást. A xanténeket, színezékként és

pigmentként történő alkalmazhatóságuk mellett, különböző területeken, többek között az orvostudományban való potenciális alkalmazásuk miatt is tanulmányozták, ahol rákellenes vagy más terápiás szerekként is használhatók lehetnek. Ezek a vegyületek kiindulópontként szolgálhatnak további gyógyszerkémiail elemzésekhez, melyek célja aktivitásuk javítása és potenciális terápiás alkalmazásuk vizsgálata.

8. Acknowledgment

I would like to express my gratitude to my supervisor, Prof. Lajos Haracska, for providing me the opportunity to join his lab as a Ph.D. student and for always being there to support me academically and morally throughout my Ph.D. journey. I am sincerely thankful to Dr. Gabriel Fenteany for mentoring and guiding me with invaluable scientific advice. Throughout the entirety of the project, his helpful supervision and advice from his years of experience proved to be beneficial. I am grateful to have received his encouragement and helpful comments, both of which have been extremely beneficial to the development of my scientific abilities.

I would also like to thank all of my lab and Delta Bio 2000 Ltd. company members: Dr. Ernő Kiss, Dr. Paras Gaur, Dr. Lili Hegedűs, Katalin Illésné Kovács, Kata Dudás, Alexandra Gráf, Ádám Sánta, Dr. Mónika Krisztina Mórocz, Katalin Vincze-Kontár, Gabriella Tick and Lajos Pintér for their technical support on my duration of Ph.D.

I am grateful to Prof. Tamás Martinek and Dr. Edit Wéber from the Department of Medicinal Chemistry, University of Szeged, Hungary, for their successful scientific collaborations and publications.

I would like to thank Dr. Viktor Honti and Dr. Gerda Szakonyi for reviewing my Ph.D. thesis and for their insightful comments and suggestions.

Last but not least, I would like to express my utmost gratitude to my family for always supporting and tolerating me throughout life and to all of my friends (Ádám Anderle, Neha Sahu, Paras Gaur, Kamal Kant, Attila Tököli, Chetna Tyagi, Tamás Marik to name a few) for making my stay in Hungary memorable.

This work received funding from the European Union's Horizon 2020 research and innovation program under grant agreement No. 739593. This research was also supported by the National Research, Development, and Innovation Office (PharmaLab, RRF-2.3.1-21-2022-00015, and TKP-31-8/PALY-2021).

9. References

- An, H., Statsyuk, A.V., 2015. An inhibitor of ubiquitin conjugation and aggresome formation. *Chem. Sci.* 6, 5235–5245. <https://doi.org/10.1039/C5SC01351H>
- An, H., Statsyuk, A.V., 2013. Development of Activity-Based Probes for Ubiquitin and Ubiquitin-like Protein Signaling Pathways. *J. Am. Chem. Soc.* 135, 16948–16962. <https://doi.org/10.1021/ja4099643>
- Bailly, V., Lamb, J., Sung, P., Prakash, S., Prakash, L., 1994. Specific complex formation between yeast RAD6 and RAD18 proteins: a potential mechanism for targeting RAD6 ubiquitin-conjugating activity to DNA damage sites. *Genes Dev.* 8, 811–820. <https://doi.org/10.1101/gad.8.7.811>
- Bailly, V., Prakash, S., Prakash, L., 1997. Domains required for dimerization of yeast Rad6 ubiquitin-conjugating enzyme and Rad18 DNA binding protein. *Mol Cell Biol* 17, 4536–4543. <https://doi.org/10.1128/MCB.17.8.4536>
- Berndsen, C.E., Wolberger, C., 2014. New insights into ubiquitin E3 ligase mechanism. *Nat Struct Mol Biol* 21, 301–307. <https://doi.org/10.1038/nsmb.2780>
- Branzei, D., Szakal, B., 2017. Building up and breaking down: mechanisms controlling recombination during replication. *Critical Reviews in Biochemistry and Molecular Biology* 52, 381–394. <https://doi.org/10.1080/10409238.2017.1304355>
- Branzei, D., Szakal, B., 2016. DNA damage tolerance by recombination: Molecular pathways and DNA structures. *DNA Repair* 44, 68–75. <https://doi.org/10.1016/j.dnarep.2016.05.008>
- Dieckman, L.M., Freudenthal, B.D., Washington, M.T., 2012. PCNA Structure and Function: Insights from Structures of PCNA Complexes and Post-

translationally Modified PCNA, in: MacNeill, S. (Ed.), *The Eukaryotic Replisome: A Guide to Protein Structure and Function*, Subcellular Biochemistry. Springer Netherlands, Dordrecht, pp. 281–299.

https://doi.org/10.1007/978-94-007-4572-8_15

Fenteany, G., Gaur, P., Hegedűs, L., Dudás, K., Kiss, E., Wéber, E., Hackler, L., Martinek, T., Puskás, L.G., Haracska, L., 2019. Multilevel structure–activity profiling reveals multiple green tea compound families that each modulate ubiquitin-activating enzyme and ubiquitination by a distinct mechanism. *Sci Rep* 9, 12801. <https://doi.org/10.1038/s41598-019-48888-6>

Fenteany, G., Gaur, P., Sharma, G., Pintér, L., Kiss, E., Haracska, L., 2020. Robust high-throughput assays to assess discrete steps in ubiquitination and related cascades. *BMC Mol and Cell Biol* 21, 21. <https://doi.org/10.1186/s12860-020-00262-5>

Gallo, D., Brown, G.W., 2019. Post-replication repair: Rad5/HLTF regulation, activity on undamaged templates, and relationship to cancer. *Critical Reviews in Biochemistry and Molecular Biology* 54, 301–332. <https://doi.org/10.1080/10409238.2019.1651817>

Ghahsare, A.G., Nazifi, Z.S., Nazifi, S.M.R., 2020. Structure-Bioactivity Relationship Study of Xanthene Derivatives: A Brief Review. *COS* 16, 1071–1077. <https://doi.org/10.2174/1570179416666191017094908>

Guan, J., Zheng, X., 2019. NEDDylation regulates RAD18 ubiquitination and localization in response to oxidative DNA damage. *Biochemical and Biophysical Research Communications* 508, 1240–1244. <https://doi.org/10.1016/j.bbrc.2018.12.072>

- Hann, Z.S., Ji, C., Olsen, S.K., Lu, X., Lux, M.C., Tan, D.S., Lima, C.D., 2019. Structural basis for adenylation and thioester bond formation in the ubiquitin E1. *Proc Natl Acad Sci USA* 116, 15475–15484. <https://doi.org/10.1073/pnas.1905488116>
- Haynes, B., Gajan, A., Nangia-Makker, P., Shekhar, M.P., 2020. RAD6B is a major mediator of triple negative breast cancer cisplatin resistance: Regulation of translesion synthesis/Fanconi anemia crosstalk and BRCA1 independence. *Biochimica et Biophysica Acta (BBA) - Molecular Basis of Disease* 1866, 165561. <https://doi.org/10.1016/j.bbadis.2019.165561>
- Haynes, B., Saadat, N., Myung, B., Shekhar, M.P.V., 2015. Crosstalk between translesion synthesis, Fanconi anemia network, and homologous recombination repair pathways in interstrand DNA crosslink repair and development of chemoresistance. *Mutation Research/Reviews in Mutation Research* 763, 258–266. <https://doi.org/10.1016/j.mrrev.2014.11.005>
- Haynes, B., Zhang, Y., Liu, F., Li, J., Petit, S., Kothayer, H., Bao, X., Westwell, A.D., Mao, G., Shekhar, M.P.V., 2016. Gold nanoparticle conjugated Rad6 inhibitor induces cell death in triple negative breast cancer cells by inducing mitochondrial dysfunction and PARP-1 hyperactivation: Synthesis and characterization. *Nanomedicine: Nanotechnology, Biology and Medicine* 12, 745–757. <https://doi.org/10.1016/j.nano.2015.10.010>
- Hedglin, M., Benkovic, S.J., 2015. Regulation of Rad6/Rad18 Activity During DNA Damage Tolerance. *Annu. Rev. Biophys.* 44, 207–228. <https://doi.org/10.1146/annurev-biophys-060414-033841>
- Hibbert, R.G., Huang, A., Boelens, R., Sixma, T.K., 2011. E3 ligase Rad18 promotes monoubiquitination rather than ubiquitin chain formation by E2 enzyme Rad6.

Proceedings of the National Academy of Sciences 108, 5590–5595.

<https://doi.org/10.1073/pnas.1017516108>

Hoege, C., Pfander, B., Moldovan, G.-L., Pyrowolakis, G., Jentsch, S., 2002. RAD6-dependent DNA repair is linked to modification of PCNA by ubiquitin and SUMO. *Nature* 419, 135–141. <https://doi.org/10.1038/nature00991>

Hong, J., Luesch, H., 2012. Largazole: From discovery to broad-spectrum therapy. *Nat. Prod. Rep.* 29, 449. <https://doi.org/10.1039/c2np00066k>

Huang, A., Hibbert, R.G., de Jong, R.N., Das, D., Sixma, T.K., Boelens, R., 2011. Symmetry and Asymmetry of the RING–RING Dimer of Rad18. *Journal of Molecular Biology* 410, 424–435. <https://doi.org/10.1016/j.jmb.2011.04.051>

Hwang, C.-S., Shemorry, A., Auerbach, D., Varshavsky, A., 2010. The N-end rule pathway is mediated by a complex of the RING-type Ubr1 and HECT-type Ufd4 ubiquitin ligases. *Nat Cell Biol* 12, 1177–1185. <https://doi.org/10.1038/ncb2121>

Hwang, W.W., Venkatasubrahmanyam, S., Ianculescu, A.G., Tong, A., Boone, C., Madhani, H.D., 2003. A Conserved RING Finger Protein Required for Histone H2B Monoubiquitination and Cell Size Control. *Molecular Cell* 11, 261–266. [https://doi.org/10.1016/S1097-2765\(02\)00826-2](https://doi.org/10.1016/S1097-2765(02)00826-2)

Hyer, M.L., Milhollen, M.A., Ciavarri, J., Fleming, P., Traore, T., Sappal, D., Huck, J., Shi, J., Gavin, J., Brownell, J., Yang, Y., Stringer, B., Griffin, R., Bruzzese, F., Soucy, T., Duffy, J., Rabino, C., Riceberg, J., Hoar, K., Lublinsky, A., Menon, S., Sintchak, M., Bump, N., Pulukuri, S.M., Langston, S., Tirrell, S., Kuranda, M., Veiby, P., Newcomb, J., Li, P., Wu, J.T., Powe, J., Dick, L.R., Greenspan, P., Galvin, K., Manfredi, M., Claiborne, C., Amidon, B.S., Bence, N.F., 2018. A

- small-molecule inhibitor of the ubiquitin activating enzyme for cancer treatment. *Nat Med* 24, 186–193. <https://doi.org/10.1038/nm.4474>
- Kanao, R., Masutani, C., 2017. Regulation of DNA damage tolerance in mammalian cells by post-translational modifications of PCNA. *Mutation Research/Fundamental and Molecular Mechanisms of Mutagenesis* 803–805, 82–88. <https://doi.org/10.1016/j.mrfmmm.2017.06.004>
- Komander, D., Rape, M., 2012. The Ubiquitin Code. *Annu. Rev. Biochem.* 81, 203–229. <https://doi.org/10.1146/annurev-biochem-060310-170328>
- Leung, W., Baxley, R., Moldovan, G.-L., Bielinsky, A.-K., 2018. Mechanisms of DNA Damage Tolerance: Post-Translational Regulation of PCNA. *Genes* 10, 10. <https://doi.org/10.3390/genes10010010>
- Lindahl, T., 1993. Instability and decay of the primary structure of DNA. *Nature* 362, 709–715. <https://doi.org/10.1038/362709a0>
- Lu, X., Olsen, S.K., Capili, A.D., Cisar, J.S., Lima, C.D., Tan, D.S., 2010. Designed Semisynthetic Protein Inhibitors of Ub/Ubl E1 Activating Enzymes. *J. Am. Chem. Soc.* 132, 1748–1749. <https://doi.org/10.1021/ja9088549>
- Lv, Z., Williams, K.M., Yuan, L., Atkison, J.H., Olsen, S.K., 2018. Crystal structure of a human ubiquitin E1–ubiquitin complex reveals conserved functional elements essential for activity. *Journal of Biological Chemistry* 293, 18337–18352. <https://doi.org/10.1074/jbc.RA118.003975>
- Maia, M., Resende, D.I.S.P., Durães, F., Pinto, M.M.M., Sousa, E., 2021. Xanthenes in Medicinal Chemistry – Synthetic strategies and biological activities. *European Journal of Medicinal Chemistry* 210, 113085. <https://doi.org/10.1016/j.ejmech.2020.113085>

- Majka, J., Burgers, P.M.J., 2004. The PCNA–RFC Families of DNA Clamps and Clamp Loaders, in: *Progress in Nucleic Acid Research and Molecular Biology*. Elsevier, pp. 227–260. [https://doi.org/10.1016/S0079-6603\(04\)78006-X](https://doi.org/10.1016/S0079-6603(04)78006-X)
- Masuda, Y., Suzuki, M., Kawai, H., Suzuki, F., Kamiya, K., 2012. Asymmetric nature of two subunits of RAD18, a RING-type ubiquitin ligase E3, in the human RAD6A–RAD18 ternary complex. *Nucleic Acids Research* 40, 1065–1076. <https://doi.org/10.1093/nar/gkr805>
- Miyase, S., Tateishi, S., Watanabe, K., Tomita, K., Suzuki, K., Inoue, H., Yamaizumi, M., 2005. Differential Regulation of Rad18 through Rad6-dependent Mono- and Polyubiquitination. *Journal of Biological Chemistry* 280, 515–524. <https://doi.org/10.1074/jbc.M409219200>
- Notenboom, V., Hibbert, R.G., van Rossum-Fikkert, S.E., Olsen, J.V., Mann, M., Sixma, T.K., 2007. Functional characterization of Rad18 domains for Rad6, ubiquitin, DNA binding and PCNA modification. *Nucleic Acids Research* 35, 5819–5830. <https://doi.org/10.1093/nar/gkm615>
- Park, J.M., Yang, S.W., Yu, K.R., Ka, S.H., Lee, S.W., Seol, J.H., Jeon, Y.J., Chung, C.H., 2014. Modification of PCNA by ISG15 Plays a Crucial Role in Termination of Error-Prone Translesion DNA Synthesis. *Molecular Cell* 54, 626–638. <https://doi.org/10.1016/j.molcel.2014.03.031>
- Rao, K.S., 1993. Genomic damage and its repair in young and aging brain. *Mol Neurobiol* 7, 23–48. <https://doi.org/10.1007/BF02780607>
- Ripley, B.M., Gildenberg, M.S., Washington, M.T., 2020. Control of DNA Damage Bypass by Ubiquitylation of PCNA. *Genes* 11, 138. <https://doi.org/10.3390/genes11020138>

- Robzyk, K., Recht, J., Osley, M.A., 2000. Rad6-Dependent Ubiquitination of Histone H2B in Yeast. *Science* 287, 501–504.
<https://doi.org/10.1126/science.287.5452.501>
- Saadat, N., Liu, F., Haynes, B., Nangia-Makker, P., Bao, X., Li, J., Polin, L.A., Gupta, S., Mao, G., Shekhar, M.P., 2018. Nano-delivery of *RAD6* /Translesion Synthesis Inhibitor SMI#9 for Triple-negative Breast Cancer Therapy. *Mol Cancer Ther* 17, 2586–2597. <https://doi.org/10.1158/1535-7163.MCT-18-0364>
- Saha, P., Mandal, T., Talukdar, A.D., Kumar, D., Kumar, S., Tripathi, P.P., Wang, Q., Srivastava, A.K., 2021. DNA polymerase eta: A potential pharmacological target for cancer therapy. *J Cell Physiol* 236, 4106–4120.
<https://doi.org/10.1002/jcp.30155>
- Sanders, M.A., Braheemi, G., Nangia-Makker, P., Balan, V., Morelli, M., Kothayer, H., Westwell, A.D., Shekhar, M.P.V., 2013. Novel Inhibitors of Rad6 Ubiquitin Conjugating Enzyme: Design, Synthesis, Identification, and Functional Characterization. *Mol Cancer Ther* 12, 373–383. <https://doi.org/10.1158/1535-7163.MCT-12-0793>
- Sanders, M.A., Haynes, B., Nangia-Makker, P., Polin, L.A., Shekhar, M.P., 2017. Pharmacological targeting of RAD6 enzyme-mediated translesion synthesis overcomes resistance to platinum-based drugs. *Journal of Biological Chemistry* 292, 10347–10363. <https://doi.org/10.1074/jbc.M117.792192>
- Schulman, B.A., Wade Harper, J., 2009. Ubiquitin-like protein activation by E1 enzymes: the apex for downstream signalling pathways. *Nat Rev Mol Cell Biol* 10, 319–331. <https://doi.org/10.1038/nrm2673>
- Sekizawa, R., Ikeno, S., Nakamura, H., Naganawa, H., Matsui, S., Iinuma, H., Takeuchi, T., 2002. Panepophenanthrin, from a Mushroom Strain, a Novel

- Inhibitor of the Ubiquitin-Activating Enzyme. *J. Nat. Prod.* 65, 1491–1493.
<https://doi.org/10.1021/np020098q>
- Slade, D., 2018. Maneuvers on PCNA Rings during DNA Replication and Repair. *Genes* 9, 416. <https://doi.org/10.3390/genes9080416>
- Sriram, S.M., Kim, B.Y., Kwon, Y.T., 2011. The N-end rule pathway: emerging functions and molecular principles of substrate recognition. *Nat Rev Mol Cell Biol* 12, 735–747. <https://doi.org/10.1038/nrm3217>
- Stukenberg, P.T., Studwell-Vaughan, P.S., O'Donnell, M., 1991. Mechanism of the sliding beta-clamp of DNA polymerase III holoenzyme. *Journal of Biological Chemistry* 266, 11328–11334. [https://doi.org/10.1016/S0021-9258\(18\)99166-0](https://doi.org/10.1016/S0021-9258(18)99166-0)
- Tsukamoto, S., Hirota, H., Imachi, M., Fujimuro, M., Onuki, H., Ohta, T., Yokosawa, H., 2005. Himeic acid A: a new ubiquitin-activating enzyme inhibitor isolated from a marine-derived fungus, *Aspergillus* sp. *Bioorganic & Medicinal Chemistry Letters* 15, 191–194. <https://doi.org/10.1016/j.bmcl.2004.10.012>
- Ungermannova, D., Lee, J., Zhang, G., Dallmann, H.G., McHenry, C.S., Liu, X., 2013. High-Throughput Screening AlphaScreen Assay for Identification of Small-Molecule Inhibitors of Ubiquitin E3 Ligase SCF^{Skp2-Cks1}. *J Biomol Screen* 18, 910–920. <https://doi.org/10.1177/1087057113485789>
- Ungermannova, D., Parker, S.J., Nasveschuk, C.G., Chapnick, D.A., Phillips, A.J., Kuchta, R.D., Liu, X., 2012a. Identification and Mechanistic Studies of a Novel Ubiquitin E1 Inhibitor. *J Biomol Screen* 17, 421–434.
<https://doi.org/10.1177/1087057111433843>
- Ungermannova, D., Parker, S.J., Nasveschuk, C.G., Wang, W., Quade, B., Zhang, G., Kuchta, R.D., Phillips, A.J., Liu, X., 2012b. Largazole and Its Derivatives

- Selectively Inhibit Ubiquitin Activating Enzyme (E1). *PLoS ONE* 7, e29208.
<https://doi.org/10.1371/journal.pone.0029208>
- Vaisman, A., Woodgate, R., 2017. Translesion DNA polymerases in eukaryotes: what makes them tick? *Critical Reviews in Biochemistry and Molecular Biology* 52, 274–303. <https://doi.org/10.1080/10409238.2017.1291576>
- Wenzel, D.M., Stoll, K.E., Klevit, R.E., 2011. E2s: structurally economical and functionally replete. *Biochemical Journal* 433, 31–42.
<https://doi.org/10.1042/BJ20100985>
- Wilkinson, N.A., Mnuskin, K.S., Ashton, N.W., Woodgate, R., 2020. Ubiquitin and Ubiquitin-Like Proteins Are Essential Regulators of DNA Damage Bypass. *Cancers* 12, 2848. <https://doi.org/10.3390/cancers12102848>
- Wood, A., Krogan, N.J., Dover, J., Schneider, J., Heidt, J., Boateng, M.A., Dean, K., Golshani, A., Zhang, Y., Greenblatt, J.F., Johnston, M., Shilatifard, A., 2003. Bre1, an E3 Ubiquitin Ligase Required for Recruitment and Substrate Selection of Rad6 at a Promoter. *Molecular Cell* 11, 267–274.
[https://doi.org/10.1016/S1097-2765\(02\)00802-X](https://doi.org/10.1016/S1097-2765(02)00802-X)
- Xu, G.W., Ali, M., Wood, T.E., Wong, D., Maclean, N., Wang, X., Gronda, M., Skrtic, M., Li, X., Hurren, R., Mao, X., Venkatesan, M., Zavareh, R.B., Ketela, T., Reed, J.C., Rose, D., Moffat, J., Batey, R.A., Dhe-Paganon, S., Schimmer, A.D., 2010. The ubiquitin-activating enzyme E1 as a therapeutic target for the treatment of leukemia and multiple myeloma. *Blood* 115, 2251–2259.
<https://doi.org/10.1182/blood-2009-07-231191>
- Yamanokuchi, R., Imada, K., Miyazaki, M., Kato, H., Watanabe, T., Fujimuro, M., Saeki, Y., Yoshinaga, S., Terasawa, H., Iwasaki, N., Rotinsulu, H., Losung, F., Mangindaan, R.E.P., Namikoshi, M., de Voogd, N.J., Yokosawa, H.,

- Tsukamoto, S., 2012. Hyrtioreticulins A–E, indole alkaloids inhibiting the ubiquitin-activating enzyme, from the marine sponge *Hyrtios reticulatus*. *Bioorganic & Medicinal Chemistry* 20, 4437–4442.
<https://doi.org/10.1016/j.bmc.2012.05.044>
- Yang, K., Weinacht, C.P., Zhuang, Z., 2013. Regulatory role of ubiquitin in eukaryotic DNA translesion synthesis. *Biochemistry* 52, 3217–3228.
<https://doi.org/10.1021/bi400194r>
- Yang, W., Gao, Y., 2018. Translesion and Repair DNA Polymerases: Diverse Structure and Mechanism. *Annu. Rev. Biochem.* 87, 239–261.
<https://doi.org/10.1146/annurev-biochem-062917-012405>
- Yang, Y., Kitagaki, J., Dai, R.-M., Tsai, Y.C., Lorick, K.L., Ludwig, R.L., Pierre, S.A., Jensen, J.P., Davydov, I.V., Oberoi, P., Li, C.-C.H., Kenten, J.H., Beutler, J.A., Vousden, K.H., Weissman, A.M., 2007. Inhibitors of Ubiquitin-Activating Enzyme (E1), a New Class of Potential Cancer Therapeutics. *Cancer Research* 67, 9472–9481. <https://doi.org/10.1158/0008-5472.CAN-07-0568>
- Yao, N., Turner, J., Kelman, Z., Stukenberg, P.T., Dean, F., Shechter, D., Pan, Z., Hurwitz, J., O'Donnell, M., 1996. Clamp loading, unloading and intrinsic stability of the PCNA, β and gp45 sliding clamps of human, *E. coli* and T4 replicases. *Genes to Cells* 1, 101–113. <https://doi.org/10.1046/j.1365-2443.1996.07007.x>
- Zeman, M.K., Lin, J.-R., Freire, R., Cimprich, K.A., 2014. DNA damage-specific deubiquitination regulates Rad18 functions to suppress mutagenesis. *Journal of Cell Biology* 206, 183–197. <https://doi.org/10.1083/jcb.201311063>
- Zhang, S., Zhou, T., Wang, Z., Yi, F., Li, C., Guo, W., Xu, H., Cui, H., Dong, X., Liu, J., Song, X., Cao, L., 2021. Post-Translational Modifications of PCNA in

Control of DNA Synthesis and DNA Damage Tolerance-the Implications in
Carcinogenesis. *Int. J. Biol. Sci.* 17, 4047–4059.

<https://doi.org/10.7150/ijbs.64628>

10. List of Publications

MTMT number: 10074814

1. Mandatory peer-reviewed international publications for the fulfilment of the doctoral process and on which this thesis is based:

1. Gabriel Fenteany*, **Gaurav Sharma***, Paras Gaur, Attila Borics, Edit Wéber, Ernő Kiss, and Lajos Haracska (2022). A series of xanthenes inhibiting Rad6 function and Rad6–Rad18 interaction in the PCNA ubiquitination cascade. *iScience* <https://doi.org/10.1016/j.isci.2022.104053> (***shared first authors**)
IF: 5.74
2. *Fenteany, G., *Gaur, P., **Sharma, G.**, Pintér, L., Kiss, E., & Haracska, L. (2020). Robust high-throughput assays to assess discrete steps in ubiquitination and related cascades. **BMC Molecular and Cell Biology**, 21(1). <https://doi.org/10.1186/s12860-020-00262-5> (*shared first authors) **IF: 3.227**

2. Other scientific work

1. Straub days 2022 (Poster presentation)
2. EMBO chemical biology workshop, Heidelberg, September 2022 (Poster presentation). Title: High-throughput screening for small molecule inhibitors of the PCNA ubiquitination cascade
3. HCEMM PhD-Postdoc symposium, Eger, Hungary, November 2022 (Poster presentation). Title: Discovery of small-molecule inhibitors of Rad6 function and the Rad6-Rad18 interaction
4. Attended 10th CEGSDM (Central European Genome Stability and DNA Repair Meeting) in Bratislava, Slovakia, 26th-27th September 2019

11. Declaration

I declare that the data used in the thesis written by Gaurav Sharma reflect the contribution of the doctoral candidate to the article: “Gabriel Fenteany*, **Gaurav Sharma***, Paras Gaur, Attila Borics, Edit Wéber, Ernő Kiss, and Lajos Haracska (2022). A series of xanthenes inhibiting Rad6 function and Rad6–Rad18 interaction in the PCNA ubiquitination cascade. *iScience* <https://doi.org/10.1016/j.isci.2022.104053> (***shared first authors**) **IF: 5.74**” and “*Fenteany, G., *Gaur, P., Sharma, G., Pintér, L., Kiss, E., & Haracska, L. (2020). Robust high-throughput assays to assess discrete steps in ubiquitination and related cascades. *BMC Molecular and Cell Biology*, 21(1). <https://doi.org/10.1186/s12860-020-00262-5> (**Co-author**) **IF:3.227**” The results reported in the Ph.D. thesis and the publication were not used to acquire any Ph.D. degree previously. I further declare that the candidate has made a significant contribution to the creation of the above-mentioned publication.

Szeged, 06 March 2023

Lajos Haracska Ph.D., D.Sc.

12. Co-authors Declaration

I declare that the data used in the thesis written by Gaurav Sharma reflect the contribution of the doctoral candidate to the article: “Gabriel Fenteany*, **Gaurav Sharma***, Paras Gaur, Attila Borics, Edit Wéber, Ernő Kiss, and Lajos Haracska (2022). A series of xanthenes inhibiting Rad6 function and Rad6–Rad18 interaction in the PCNA ubiquitination cascade. *iScience* <https://doi.org/10.1016/j.isci.2022.104053> (***shared first authors**) **IF: 5.74**” and “*Fenteany, G., *Gaur, P., **Sharma, G.**, Pintér, L., Kiss, E., & Haracska, L. (2020). Robust high-throughput assays to assess discrete steps in ubiquitination and related cascades. *BMC Molecular and Cell Biology*, 21(1). <https://doi.org/10.1186/s12860-020-00262-5> (**Co-author**) **IF:3.227**”

The results reported in the Ph.D. thesis and the publications were not used to acquire any Ph.D. degree previously. I further declare that the candidate has made a significant contribution to the creation of the above-mentioned publications.

Szeged, 06 March 2023

A handwritten signature in black ink, appearing to read 'Gabriel Fenteany'.

Gabriel Fenteany, Ph.D.

13. Appendix

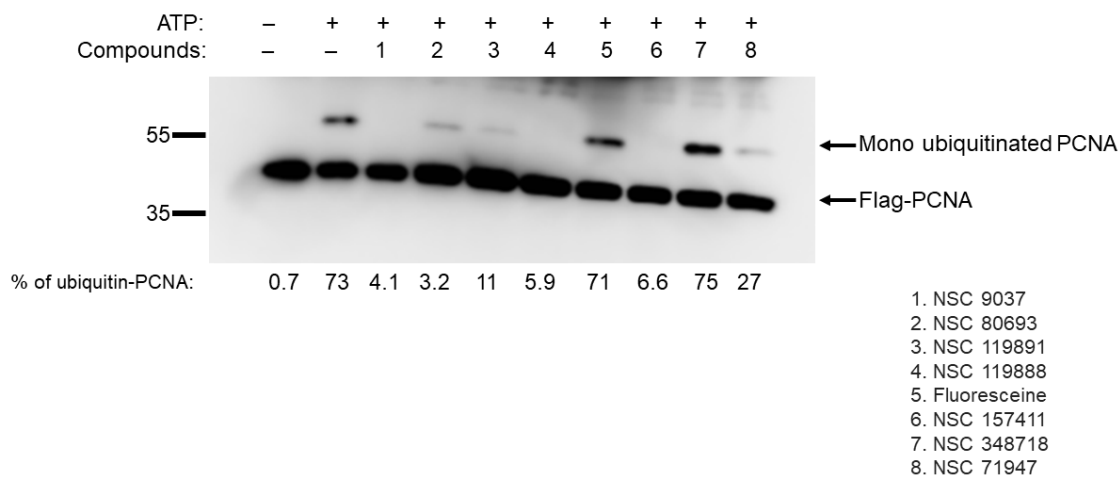


Figure S1 Western blot analysis showing PCNA ubiquitination, related to Figure 9. Western blot analysis was carried out to confirm the inhibition of PCNA ubiquitination by the compounds at a final concentration of 100 mM. Final DMSO concentration in all control and experimental samples was 1% in this and subsequent figures.

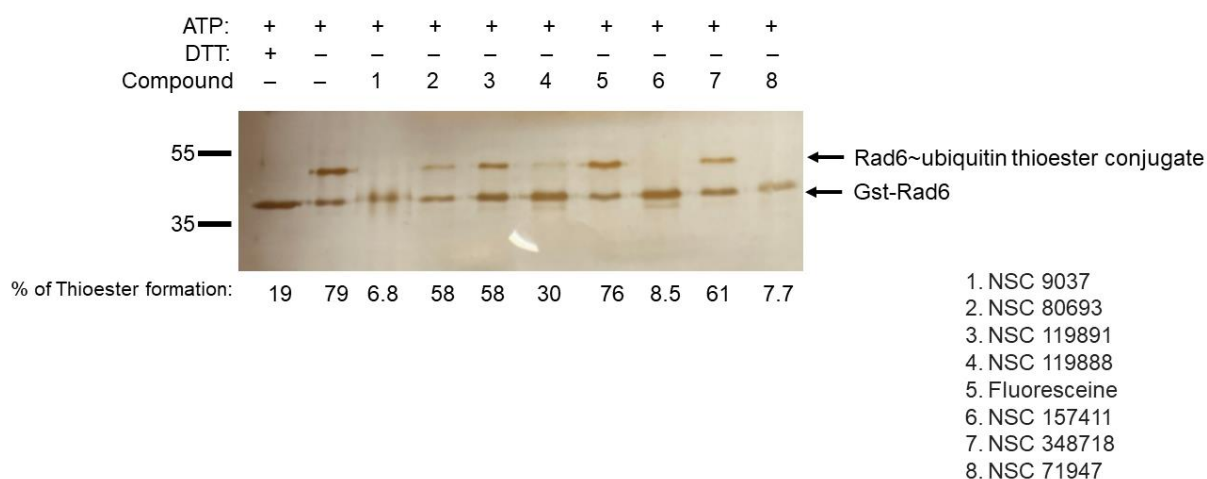
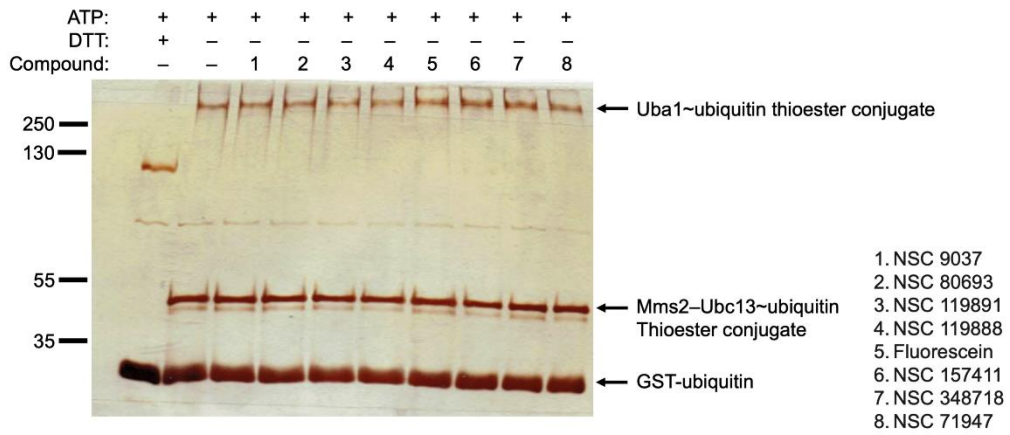


Figure S2 Silver-stained gel showing Rad6~ubiquitin thioester formation, related to Figure 10.

Silver staining was done to investigate Rad6~ubiquitin thioester formation in the presence of compounds at a final concentration of 100 mM.

A



B

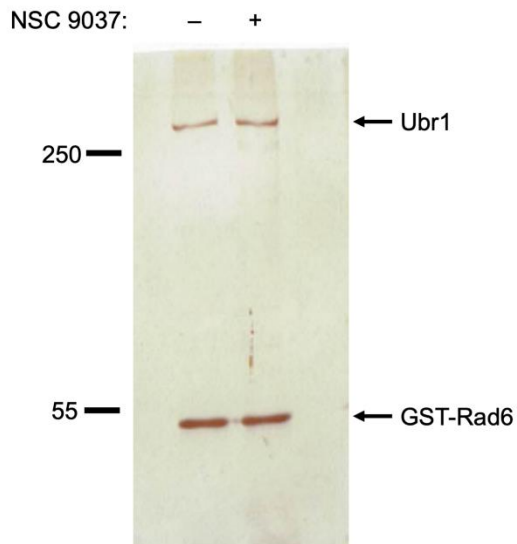


Figure S3 Effect of compounds on Mms2-Ubc13-ubiquitin and Uba1~ubiquitin thioester formation and Rad6-Ubr1 interaction in pulldown assay, related to Figure 14. (A) Effect of compounds on Mms2 -- Ubc13~ubiquitin and Uba1~ubiquitin thioester formation. Stained gel of proteins following compound treatments at a final concentration of 100 mM is shown. (B) Pulldown of Rad6 with Ubr1, another E3 ubiquitin ligase in the presence and absence of NSC 9037 (100 m M).

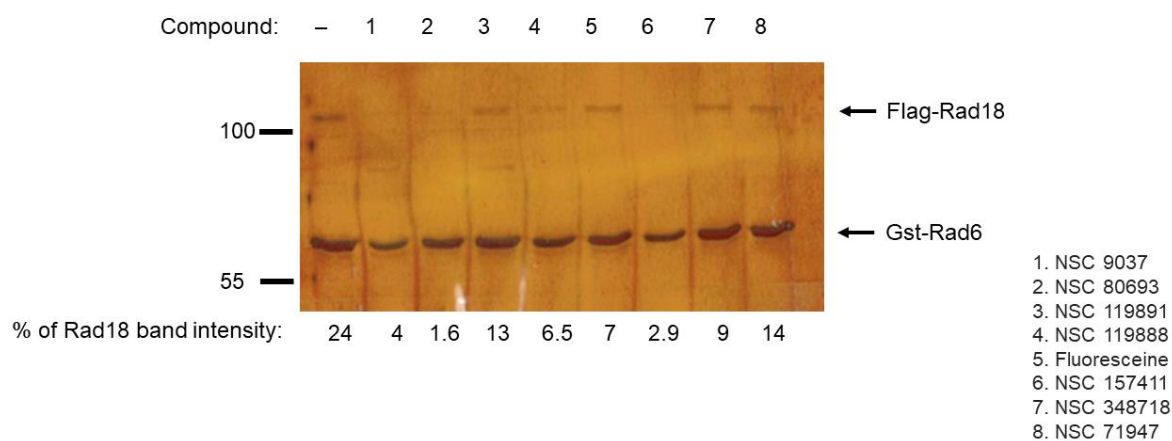


Figure S4 Rad6-Rad18 pulldown assay, related to Figure 13.

Pulldown of Rad6-Rad18 was carried out as an alternative approach to test possible inhibition of the interaction of these two proteins with compounds at a final concentration of 100 mM. The percentage of Rad18 band intensity was calculated using the ImageJ software by dividing the intensity of the Rad18 band by the sum of the intensity of the Rad6 and Rad18 bands, followed by multiplying by 100.